JHEP

Published for SISSA by Springer

Received: January 14, 2016
Revised: July 8, 2016
Accepted: August 20, 2016
Published: August 24, 2016

Measurement of the CP-violating phase ϕ_s and the B_s^0 meson decay width difference with $B_s^0 \to J/\psi\phi$ decays in ATLAS

The ATLAS collaboration

E-mail: atlas.publications@cern.ch

Abstract: A measurement of the B_s^0 decay parameters in the $B_s^0 \to J/\psi\phi$ channel using an integrated luminosity of $14.3\,\text{fb}^{-1}$ collected by the ATLAS detector from 8 TeV pp collisions at the LHC is presented. The measured parameters include the CP-violating phase ϕ_s, the decay width Γ_s and the width difference between the mass eigenstates $\Delta\Gamma_s$. The values measured for the physical parameters are statistically combined with those from $4.9\,\text{fb}^{-1}$ of 7 TeV data, leading to the following:

$$\begin{aligned}\phi_s &= -0.090 \pm 0.078\ (\text{stat.}) \pm 0.041\ (\text{syst.})\ \text{rad}\\ \Delta\Gamma_s &= 0.085 \pm 0.011\ (\text{stat.}) \pm 0.007\ (\text{syst.})\ \text{ps}^{-1}\\ \Gamma_s &= 0.675 \pm 0.003\ (\text{stat.}) \pm 0.003\ (\text{syst.})\ \text{ps}^{-1}.\end{aligned}$$

In the analysis the parameter $\Delta\Gamma_s$ is constrained to be positive. Results for ϕ_s and $\Delta\Gamma_s$ are also presented as 68% and 95% likelihood contours in the ϕ_s-$\Delta\Gamma_s$ plane. Also measured in this decay channel are the transversity amplitudes and corresponding strong phases. All measurements are in agreement with the Standard Model predictions.

Keywords: B physics, CP violation, Flavor physics, Hadron-Hadron scattering (experiments)

ArXiv ePrint: 1601.03297

doi:10.1007/JHEP08(2016)147

Contents

1 Introduction 1

2 ATLAS detector and Monte Carlo simulation 2

3 Reconstruction and candidate selection 3

4 Flavour tagging 4
- 4.1 $B^{\pm} \to J/\psi K^{\pm}$ event selection 5
- 4.2 Flavour tagging methods 5
- 4.3 Using tag information in the B_s^0 fit 8

5 Maximum likelihood fit 11
- 5.1 Signal PDF 12
- 5.2 Background PDF 13
- 5.3 Muon trigger proper time-dependent efficiency 16

6 Results 16

7 Systematic uncertainties 16

8 Discussion 21

9 Combination of 7 TeV and 8 TeV results 23

10 Summary 25

The ATLAS collaboration 29

JHEP08(2016)147

1 Introduction

New phenomena beyond the predictions of the Standard Model (SM) may alter CP violation in b-hadron decays. A channel that is expected to be sensitive to new physics contributions is the decay $B_s^0 \to J/\psi\phi$. CP violation in the $B_s^0 \to J/\psi\phi$ decay occurs due to interference between direct decays and decays with B_s^0-$\bar{B}_s^0$ mixing. The oscillation frequency of B_s^0 meson mixing is characterized by the mass difference Δm_s of the heavy ($B_{\rm H}$) and light ($B_{\rm L}$) mass eigenstates. The CP violating phase ϕ_s is defined as the weak phase difference between the B_s^0-$\bar{B}_s^0$ mixing amplitude and the $b \to c\bar{c}s$ decay amplitude. In the absence of CP violation, the $B_{\rm H}$ state would correspond to the CP-odd state and the $B_{\rm L}$ to the CP-even state. In the SM the phase ϕ_s is small and can be related to Cabibbo-Kobayashi-Maskawa (CKM) quark mixing matrix elements via the relation $\phi_s \simeq -2\beta_s$,

with $\beta_s = \arg[-(V_{ts}V_{tb}^*)/(V_{cs}V_{cb}^*)]$; assuming no physics beyond the SM contributions to B_s^0 mixing and decays, a value of $-2\beta_s = -0.0363^{+0.0016}_{-0.0015}$ rad can be predicted by combining beauty and kaon physics observables [1].

Other physical quantities involved in B_s^0-$\bar{B}_s^0$ mixing are the decay width $\Gamma_s = (\Gamma_{\rm L} + \Gamma_H)/2$ and the width difference $\Delta\Gamma_s = \Gamma_{\rm L} - \Gamma_H$, where $\Gamma_{\rm L}$ and Γ_H are the decay widths of the different eigenstates. The width difference is predicted to be $\Delta\Gamma_s = 0.087 \pm 0.021$ ps^{-1} [2]. Physics beyond the SM is not expected to affect $\Delta\Gamma_s$ as significantly as ϕ_s [3]. However, extracting $\Delta\Gamma_s$ from data is interesting as it allows theoretical predictions to be tested [3]. Previous measurements of these quantities have been reported by the DØ, CDF, LHCb, ATLAS and CMS collaborations [4–9].

The decay of the pseudoscalar B_s^0 to the vector-vector $J/\psi(\mu^+\mu^-)\phi(K^+K^-)$ final state results in an admixture of CP-odd and CP-even states, with orbital angular momentum $L = 0$, 1 or 2. The final states with orbital angular momentum $L = 0$ or 2 are CP-even, while the state with $L = 1$ is CP-odd. The same final state can also be produced with K^+K^- pairs in an S-wave configuration [10]. This S-wave final state is CP-odd. The CP states are separated statistically using an angular analysis of the final-state particles. Flavour tagging is used to distinguish between the initial B_s^0 and $\bar{B}_s^0$ states.

The analysis presented here provides a measurement of the $B_s^0 \to J/\psi\phi$ decay parameters using 14.3 fb^{-1} of LHC pp data collected by the ATLAS detector during 2012 at a centre-of-mass energy of 8 TeV. This is an update of the previous flavour-tagged time-dependent angular analysis of $B_s^0 \to J/\psi\phi$ [8] that was performed using 4.9 fb^{-1} of data collected at 7 TeV. Electrons are now included, in addition to final-state muons, for the flavour tagging using leptons.

2 ATLAS detector and Monte Carlo simulation

The ATLAS detector [11] is a multi-purpose particle physics detector with a forward-backward symmetric cylindrical geometry and nearly 4π coverage in solid angle.[1] The inner tracking detector (ID) consists of a silicon pixel detector, a silicon microstrip detector and a transition radiation tracker. The ID is surrounded by a thin superconducting solenoid providing a 2 T axial magnetic field, and by a high-granularity liquid-argon (LAr) sampling electromagnetic calorimeter. A steel/scintillator tile calorimeter provides hadronic coverage in the central rapidity range. The end-cap and forward regions are instrumented with LAr calorimeters for electromagnetic and hadronic measurements. The muon spectrometer (MS) surrounds the calorimeters and consists of three large superconducting toroids with eight coils each, a system of tracking chambers, and detectors for triggering.

The muon and tracking systems are of particular importance in the reconstruction of B meson candidates. Only data collected when both these systems were operating

[1] ATLAS uses a right-handed coordinate system with its origin at the nominal interaction point (IP) in the centre of the detector and the z-axis along the beam pipe. The x-axis points from the IP to the centre of the LHC ring, and the y-axis points upward. Cylindrical coordinates (r, ϕ) are used in the transverse plane, ϕ being the azimuthal angle around the beam pipe. The pseudorapidity is defined in terms of the polar angle θ as $\eta = -\ln\tan(\theta/2)$.

JHEP08(2016)147

correctly and when the LHC beams were declared to be stable are used in the analysis. The data were collected during a period of rising instantaneous luminosity, and the trigger conditions varied over this time. The triggers used to select events for this analysis are based on identification of a $J/\psi \to \mu^+\mu^-$ decay, with transverse momentum (p_{T}) thresholds of either 4 GeV or 6 GeV for the muons. The measurement uses 14.3 fb^{-1} of pp collision data collected with the ATLAS detector at a centre-of-mass energy of 8 TeV. Data collected at the beginning of the 8 TeV data-taking period are not included in the analysis due to a problem with the trigger tracking algorithm. The trigger was subsequently changed to use a different tracking algorithm that did not have this problem.

To study the detector response, estimate backgrounds and model systematic effects, 12 million Monte Carlo (MC) simulated $B_s^0 \to J/\psi\phi$ events were generated using Pythia 8 [12, 13] tuned with ATLAS data [14]. No p_{T} cuts were applied at the generator level. The detector response was simulated using the ATLAS simulation framework based on GEANT4 [15, 16]. In order to take into account the varying number of proton-proton interactions per bunch crossing (pile-up) and trigger configurations during data-taking, the MC events were weighted to reproduce the same pile-up and trigger conditions in data. Additional samples of the background decay $B_d^0 \to J/\psi K^{0*}$, as well as the more general $b\bar{b} \to J/\psi X$ and $pp \to J/\psi X$ backgrounds were also simulated using Pythia 8.

3 Reconstruction and candidate selection

Events must pass the trigger selections described in section 2. In addition, each event must contain at least one reconstructed primary vertex, formed from at least four ID tracks, and at least one pair of oppositely charged muon candidates that are reconstructed using information from the MS and the ID [17]. A muon identified using a combination of MS and ID track parameters is referred to as a *combined-muon*. A muon formed from a MS track segment that is not associated with a MS track but is matched to an ID track extrapolated to the MS is referred to as a *segment-tagged muon*. The muon track parameters are determined from the ID measurement alone, since the precision of the measured track parameters is dominated by the ID track reconstruction in the p_{T} range of interest for this analysis. Pairs of oppositely charged muon tracks are refitted to a common vertex and the pair is accepted for further consideration if the quality of the fit meets the requirement $\chi^2/\mathrm{d.o.f.} < 10$. The invariant mass of the muon pair is calculated from the refitted track parameters. In order to account for varying mass resolution in different parts of the detector, the J/ψ candidates are divided into three subsets according to the pseudorapidity η of the muons. A maximum-likelihood fit is used to extract the J/ψ mass and the corresponding mass resolution for these three subsets. When both muons have $|\eta| < 1.05$, the dimuon invariant mass must fall in the range 2.959–3.229 GeV to be accepted as a J/ψ candidate. When one muon has $1.05 < |\eta| < 2.5$ and the other muon $|\eta| < 1.05$, the corresponding signal region is 2.913–3.273 GeV. For the third subset, where both muons have $1.05 < |\eta| < 2.5$, the signal region is 2.852–3.332 GeV. In each case the signal region is defined so as to retain 99.8% of the J/ψ candidates identified in the fits.

JHEP08(2016)147

The candidates for the decay $\phi \to K^+K^-$ are reconstructed from all pairs of oppositely charged particles with $p_{\rm T} > 1$ GeV and $|\eta| < 2.5$ that are not identified as muons. Candidate events for $B_s^0 \to J/\psi(\mu^+\mu^-)\phi(K^+K^-)$ decays are selected by fitting the tracks for each combination of $J/\psi \to \mu^+\mu^-$ and $\phi \to K^+K^-$ to a common vertex. Each of the four tracks is required to have at least one hit in the pixel detector and at least four hits in the silicon microstrip detector. The fit is further constrained by fixing the invariant mass calculated from the two muon tracks to the J/ψ mass [18]. A quadruplet of tracks is accepted for further analysis if the vertex fit has a χ^2/d.o.f. < 3, the fitted $p_{\rm T}$ of each track from $\phi \to K^+K^-$ is greater than 1 GeV and the invariant mass of the track pairs (assuming that they are kaons) falls within the interval 1.0085 GeV $< m(K^+K^-) <$ 1.0305 GeV. If there is more than one accepted candidate in the event, the candidate with the lowest χ^2/d.o.f. is selected. In total, 375,987 B_s^0 candidates are collected within a mass range of 5.150–5.650 GeV.

For each B_s^0 meson candidate the proper decay time t is estimated using the expression:

$$t = \frac{L_{xy}\ m_{_B}}{p_{{\rm T}_B}},$$

where $p_{{\rm T}_B}$ is the reconstructed transverse momentum of the B_s^0 meson candidate and $m_{_B}$ denotes the mass of the B_s^0 meson, taken from [18]. The transverse decay length, L_{xy}, is the displacement in the transverse plane of the B_s^0 meson decay vertex with respect to the primary vertex, projected onto the direction of the B_s^0 transverse momentum. The position of the primary vertex used to calculate this quantity is determined from a refit following the removal of the tracks used to reconstruct the B_s^0 meson candidate.

For the selected events the average number of pile-up proton-proton interactions is 21, necessitating a choice of the best candidate for the primary vertex at which the B_s^0 meson is produced. The variable used is the three-dimensional impact parameter d_0, which is calculated as the distance between the line extrapolated from the reconstructed B_s^0 meson vertex in the direction of the B_s^0 momentum, and each primary vertex candidate. The chosen primary vertex is the one with the smallest d_0.

A study [19] made using a MC simulated dataset has shown that the precision of the reconstructed B_s^0 proper decay time remains stable over the range of pile-up encountered during 2012 data-taking. No B_s^0 meson decay-time cut is applied in this analysis.

4 Flavour tagging

The initial flavour of a neutral B meson can be inferred using information from the opposite-side B meson that contains the other pair-produced b-quark in the event [20, 21]. This is referred to as opposite-side tagging (OST).

To study and calibrate the OST methods, events containing $B^\pm \to J/\psi K^\pm$ decays are used, where the flavour of the $B^\pm$-meson is provided by the kaon charge. A sample of $B^\pm \to J/\psi K^\pm$ candidates is selected from the entire 2012 dataset satisfying the data-quality selection described in section 2. Since the OST calibration is not affected by the trigger problem at the start of the 8 TeV data-taking period, the tagging measurement uses 19.5 fb^{-1} of integrated luminosity of pp collision data.

JHEP08(2016)147

4.1 $B^{\pm} \to J/\psi K^{\pm}$ event selection

In order to select candidate $B^{\pm} \to J/\psi K^{\pm}$ decays, firstly J/ψ candidates are selected from pairs of oppositely charged combined-muons forming a good vertex, following the criteria described in section 3. Each muon is required to have a transverse momentum of at least 4 GeV and pseudorapidity within $|\eta| < 2.5$. The invariant mass of the dimuon candidate is required to satisfy 2.8 GeV $< m(\mu^+\mu^-) <$ 3.4 GeV. To form the B candidate, an additional track, satisfying the same quality requirements described for tracks in section 3, is combined with the dimuon candidate using the charged kaon mass hypothesis, and a vertex fit is performed with the mass of the dimuon pair constrained to the known value of the J/ψ mass. To reduce the prompt component of the combinatorial background, a requirement is applied to the transverse decay length of the B candidate of $L_{xy} > 0.1$ mm.

A sideband subtraction method is used in order to study parameter distributions corresponding to the $B^{\pm}$ signal processes with the background component subtracted. Events are divided into sub-sets into five intervals in the pseudorapidity of the B candidate and three mass regions. The mass regions are defined as a signal region around the fitted peak signal mass position $\mu \pm 2\sigma$ and the sideband regions are defined as $[\mu - 5\sigma, \mu - 3\sigma]$ and $[\mu + 3\sigma, \mu + 5\sigma]$, where μ and σ are the mean and width of the Gaussian function describing the B signal mass. Separate binned extended maximum-likelihood fits are performed to the invariant mass distribution in each region of pseudorapidity.

An exponential function is used to model the combinatorial background and a hyperbolic tangent function to parameterize the low-mass contribution from incorrectly or partially reconstructed B decays. A Gaussian function is used to model the $B^{\pm} \to J/\psi\pi^{\pm}$ contribution. The contribution from non-combinatorial background is found to have a negligible effect on the tagging procedure. Figure 1 shows the invariant mass distribution of B candidates for all rapidity regions overlaid with the fit result for the combined data.

4.2 Flavour tagging methods

Several methods that differ in efficiency and discriminating power are available to infer the flavour of the opposite-side b-quark. The measured charge of a muon or electron from a semileptonic decay of the B meson provides strong separation power; however, the $b \to \ell$ transitions are diluted through neutral B meson oscillations, as well as by cascade decays $b \to c \to \ell$, which can alter the charge of the lepton relative to those from direct $b \to \ell$ decays. The separation power of lepton tagging is enhanced by considering a weighted sum of the charge of the tracks in a cone around the lepton, where the weighting function is determined separately for each tagging method by optimizing the tagging performance. If no lepton is present, a weighted sum of the charge of tracks in a jet associated with the opposite-side B meson decay provides some separation. The flavour tagging methods are described in detail below.

For muon-based tagging, an additional muon is required in the event, with $p_{\mathrm{T}} > 2.5$ GeV, $|\eta| < 2.5$ and with $|\Delta z| < 5$ mm from the primary vertex. Muons are classified according to their reconstruction class, *combined* or *segment-tagged*, and subsequently treated as

JHEP08(2016)147

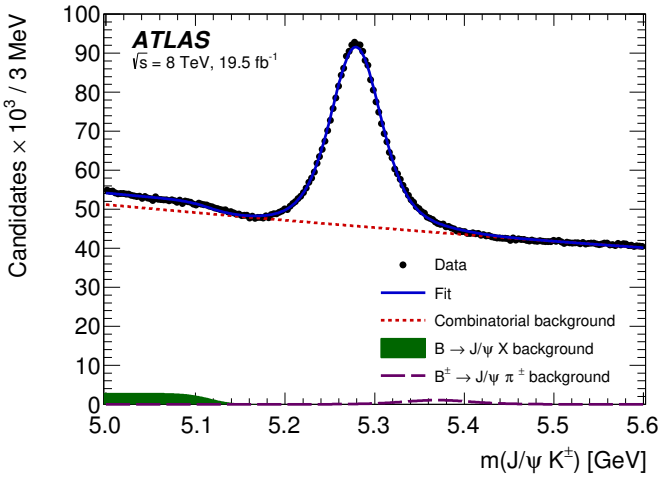

Figure 1. The invariant mass distribution for $B^{\pm} \to J/\psi K^{\pm}$ candidates satisfying the selection criteria, used to study the flavour tagging. Data are shown as points, and the overall result of the fit is given by the blue curve. The contribution from the combinatorial background component is indicated by the red dotted line, partially reconstructed B decays by the green shaded area, and decays of $B^{\pm} \to J/\psi\pi^{\pm}$, where the pion is mis-assigned a kaon mass, by the purple dashed line.

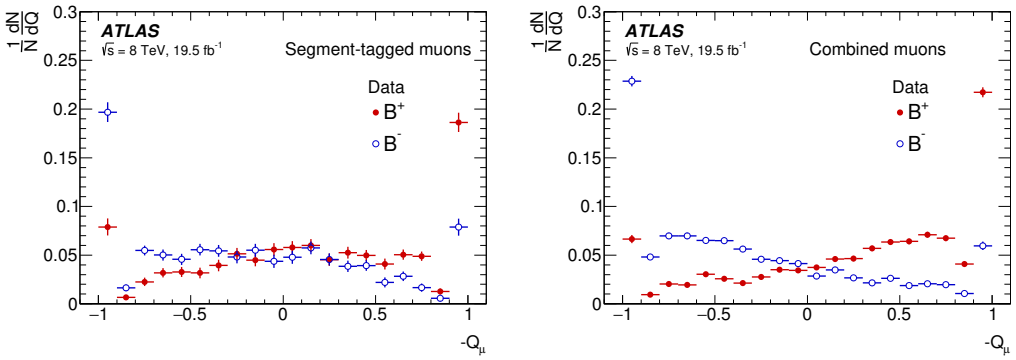

Figure 2. The opposite-side muon cone charge distribution for $B^{\pm}$ signal candidates for *segment-tagged* (left) and *combined* (right) muons. The $B^{\pm}$ charge is determined from the kaon charge.

distinct flavour tagging methods. In the case of multiple muons, the muon with the highest transverse momentum is selected.

A muon *cone charge* variable is constructed, defined as

$$Q_{\mu} = \frac{\sum_i^{N\ \text{tracks}} q_i \cdot (p_{\mathrm{T}i})^{\kappa}}{\sum_i^{N\ \text{tracks}} (p_{\mathrm{T}i})^{\kappa}},$$

where q is the charge of the track, $\kappa = 1.1$ and the sum is performed over the reconstructed ID tracks within a cone, $\Delta R = \sqrt{(\Delta\phi)^2 + (\Delta\eta)^2} < 0.5$, around the muon direction. The reconstructed ID tracks must have $p_{\mathrm{T}} > 0.5$ GeV and $|\eta| < 2.5$. Tracks associated with the $B^{\pm}$ signal decay are excluded from the sum. In figure 2 the opposite-side muon cone charge distributions are shown for candidates from $B^{\pm}$ signal decays.

JHEP08(2016)147

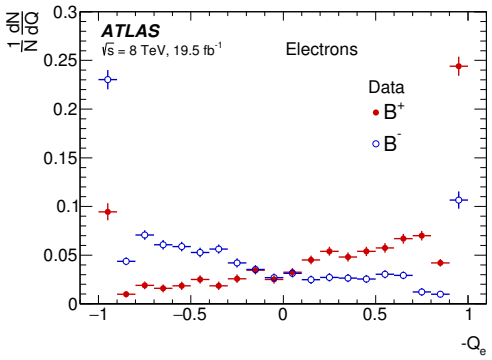

Figure 3. The opposite-side electron cone charge distribution for $B^{\pm}$ signal candidates.

For electron-based tagging, an electron is identified using information from the inner detector and calorimeter and is required to satisfy the tight electron quality criteria [22]. The inner detector track associated with the electron is required to have $p_{\mathrm{T}} > 0.5$ GeV and $|\eta| < 2.5$. It is required to pass within $|\Delta z| < 5$ mm of the primary vertex to remove electrons from non-signal interactions. To exclude electrons associated with the signal-side of the decay, electrons are rejected that have momenta within a cone of size $\Delta R = 0.4$ around the signal B candidate direction in the laboratory frame and opening angle between the B candidate and electron momenta, ζ_b, of $\cos(\zeta_b) > 0.98$. In the case of more than one electron passing the selection, the electron with the highest transverse momentum is chosen. As in the case of muon tagging, additional tracks within a cone of size $\Delta R = 0.5$ are used to form the electron cone charge Q_e with $\kappa = 1.0$. If there are no additional tracks within the cone, the charge of the electron is used. The resulting opposite-side electron cone charge distribution is shown in figure 3 for B^+ and B^- signal events.

In the absence of a muon or electron, *b-tagged* jets (i.e. jets that are the product of a b-quark) are identified using a multivariate tagging algorithm [23], which is a combination of several b-tagging algorithms using an artificial neural network and outputs a *b-tag* weight classifier. Jets are selected that exceed a *b-tag* weight of 0.7. This value is optimized to maximize the tagging power of the calibration sample. Jets are reconstructed from track information using the anti-k_t algorithm [24] with a radius parameter $R = 0.8$. In the case of multiple jets, the jet with the highest value of the b-tag weight is used.

The *jet charge* is defined as

$$Q_{\mathrm{jet}} = \frac{\sum_i^{N\ \mathrm{tracks}} q_i \cdot (p_{\mathrm{T}i})^{\kappa}}{\sum_i^{N\ \mathrm{tracks}} (p_{\mathrm{T}i})^{\kappa}},$$

where $\kappa = 1.1$ and the sum is over the tracks associated with the jet, excluding those tracks associated with a primary vertex other than that of the signal decay and tracks from the signal candidate. Figure 4 shows the distribution of the opposite-side jet-charge for $B^{\pm}$ signal candidates.

The efficiency, ϵ, of an individual tagging method is defined as the ratio of the number of events tagged by that method to the total number of candidates. A probability $P(B|Q)$ ($P(\bar{B}|Q)$) that a specific event has a signal decay containing a $\bar{b}$-quark (b-quark)

JHEP08(2016)147

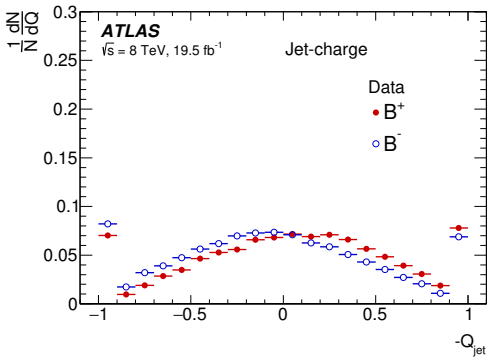

Figure 4. Opposite-side jet-charge distribution for $B^{\pm}$ signal candidates.

given the value of the discriminating variable is constructed from the calibration samples for each of the B^+ and B^- samples, which defines $P(Q|B^+)$ and $P(Q|B^-)$, respectively. The probability to tag a signal event as containing a $\bar{b}$-quark is therefore $P(B|Q) = P(Q|B^+)/(P(Q|B^+) + P(Q|B^-))$, and correspondingly $P(\bar{B}|Q) = 1 - P(B|Q)$. It is possible to define a quantity called the dilution $\mathcal{D} = P(B|Q) - P(\bar{B}|Q) = 2P(B|Q) - 1$, which represents the strength of a particular flavour tagging method. The tagging power of a particular tagging method is defined as $T = \epsilon\mathcal{D}^2 = \sum_i \epsilon_i \cdot (2P_i(B|Q_i) - 1)^2$, where the sum is over the bins of the probability distribution as a function of the charge variable. An effective dilution, $D = \sqrt{T/\epsilon}$, is calculated from the measured tagging power and efficiency.

The flavour tagging method applied to each B_s^0 candidate event is taken from the information contained in a given event. By definition there is no overlap between lepton-tagged and jet-charge-tagged events. The overlap between muon- and electron-tagged events, corresponding to 0.4% of all tagged events, is negligibly small. In the case of doubly tagged events, the tagger with the highest tagging power is selected; however, the choice of hierarchy between muon- and electron-tagged events is shown to have negligible impact on the final fit results. If it is not possible to provide a tagging response for the event, then a probability of 0.5 is assigned. A summary of the tagging performance is given in table 1.

4.3 Using tag information in the B_s^0 fit

The tag-probability for each B_s^0 candidate is determined from calibrations derived from a sample of $B^{\pm} \to J/\psi K^{\pm}$ candidates, as described in section 4.2. The distributions of tag-probabilities for the signal and background are different and since the background cannot be factorized out, additional probability terms, $P_{\rm s}(P(B|Q))$ and $P_{\rm b}(P(B|Q))$ for signal and background, respectively, are included in the fit. The distributions of tag-probabilities for the B_s^0 candidates consist of continuous and discrete parts (events with a tag charge of ± 1); these are treated separately as described below.

To describe the continuous part, a fit is first performed to the sideband data, i.e., 5.150 GeV $< m(B_s^0) <$ 5.317 GeV or 5.417 GeV $< m(B_s^0) <$ 5.650 GeV, where $m(B_s^0)$ is the mass of the B_s^0 candidate. Different functions are used for the different tagging methods. For the combined-muon tagging method, the function has the form of the sum of a

JHEP08(2016)147

Tagger	Efficiency [%]	Dilution [%]	Tagging Power [%]
Combined μ	4.12 ± 0.02	47.4 ± 0.2	0.92 ± 0.02
Electron	1.19 ± 0.01	49.2 ± 0.3	0.29 ± 0.01
Segment-tagged μ	1.20 ± 0.01	28.6 ± 0.2	0.10 ± 0.01
Jet-charge	13.15 ± 0.03	11.85 ± 0.03	0.19 ± 0.01
Total	19.66 ± 0.04	27.56 ± 0.06	1.49 ± 0.02

Table 1. Summary of tagging performance for the different flavour tagging methods described in the text. Uncertainties shown are statistical only. The efficiency and tagging power are each determined by summing over the individual bins of the charge distribution. The effective dilution is obtained from the measured efficiency and tagging power. For the efficiency, dilution, and tagging power, the corresponding uncertainty is determined by combining the appropriate uncertainties in the individual bins of each charge distribution.

fourth-order polynomial and two exponential functions. A second-order polynomial and two exponential functions are applied for the electron tagging algorithm. A sum of three Gaussian functions is used for the segment-tagged muons. For the jet-charge tagging algorithm an eighth-order polynomial is used. In all four cases unbinned maximum-likelihood fits to data are used. In the next step, the same function as applied to the sidebands is used to describe the distributions for events in the signal region: the background parameters are fixed to the values obtained from the fits to the sidebands while the signal parameters are free in this step. The ratio of background to signal (obtained from a simultaneous mass-lifetime fit) is fixed as well. The results of the fits projected onto histograms of B_s^0 tag-probability for the different tagging methods are shown in figure 5.

To account for possible deviations between data and the selected fit models a number of alternative fit functions are used to determine systematic uncertainties in the B_s^0 fit. These fit variations are described in section 7.

The discrete components of the tag-probability distribution originate from cases where the tag is derived from a single track, giving a tag charge of exactly $+1$ or -1. The fractions of events f_{+1} and f_{-1} with charges $+1$ and -1, respectively, are determined separately for signal and background using events from the same B_s^0 mass signal and sideband regions. Positive and negative charges are equally probable for background candidates formed from a random combination of a J/ψ and a pair of tracks, but this is not the case for background candidates formed from a partially reconstructed b-hadron. For signal and background contributions, similar fractions of events that are tagged with $+1$ or -1 tagging charge are observed for each of the tagging methods. The remaining fraction of events, $1 - f_{+1} - f_{-1}$, constitute the continuous part of the distributions. Table 2 summarizes the fractions f_{+1} and f_{-1} obtained for signal and background events and for the different tag methods.

To estimate the fractions of signal and background events which have tagging, a similar sideband-subtraction method is used to determine the relative fraction of signal and background events tagged using the different methods. These fractions are also included in the maximum-likelihood fit, described in section 5. The results are summarized in table 3.

JHEP08(2016)147

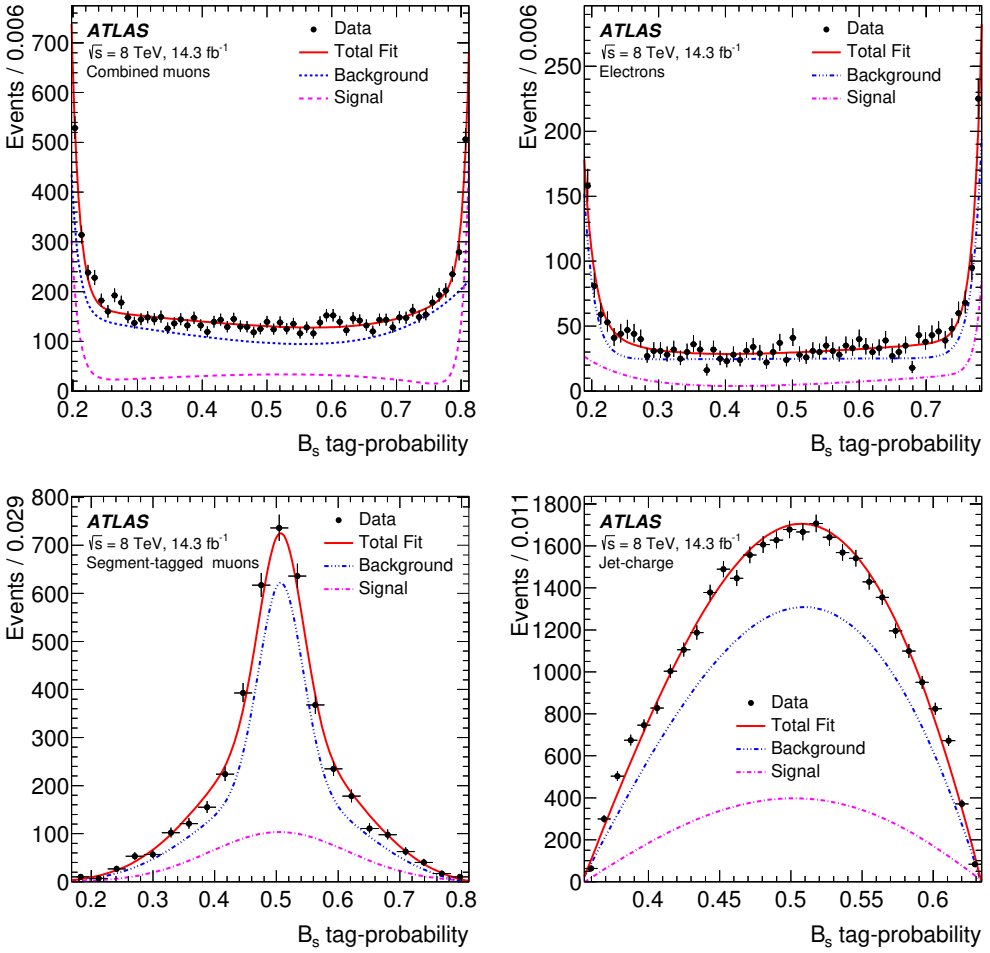

Figure 5. The continuous part of tag-probability for tagging using combined-muons (top-left), electrons (top-right), segment-tagged muons (bottom-left) and jet-charge (bottom-right). Black dots are data, blue is a fit to the sidebands, purple to the signal and red is a sum of both fits.

Tag method	Signal		Background	
	f_{+1}	f_{-1}	f_{+1}	f_{-1}
Combined μ	0.124 ± 0.012	0.127 ± 0.012	0.093 ± 0.003	0.095 ± 0.003
Electron	0.105 ± 0.020	0.139 ± 0.021	0.110 ± 0.007	0.110 ± 0.007
Segment-tagged μ	0.147 ± 0.024	0.118 ± 0.023	0.083 ± 0.004	0.084 ± 0.004
Jet-charge	0.071 ± 0.005	0.069 ± 0.005	0.068 ± 0.002	0.069 ± 0.002

Table 2. Table summarizing the fraction of events f_{+1} and f_{-1} with tag charges of $+1$ and -1, respectively for signal and background events and for the different tag methods. Only statistical errors are quoted.

JHEP08(2016)147

Tag method	Signal	Background
Combined μ	0.047 ± 0.003	0.038 ± 0.001
Electron	0.012 ± 0.001	0.008 ± 0.001
Segment-tagged μ	0.013 ± 0.001	0.015 ± 0.001
Jet-charge	0.135 ± 0.003	0.100 ± 0.001
Untagged	0.793 ± 0.002	0.839 ± 0.002

Table 3. Table summarizing the relative fractions of signal and background events tagged using the different tag methods. The fractions include both the continuous and discrete contributions. Only statistical errors are quoted.

5 Maximum likelihood fit

An unbinned maximum-likelihood fit is performed on the selected events to extract the parameter values of the $B_s^0 \to J/\psi(\mu^+\mu^-)\phi(K^+K^-)$ decay. The fit uses information about the reconstructed mass m, the measured proper decay time t, the measured proper decay time uncertainty σ_t, the tagging probability, and the transversity angles Ω of each $B_s^0 \to J/\psi\phi$ decay candidate. The measured proper decay time uncertainty σ_t is calculated from the covariance matrix associated with the vertex fit of each candidate event. The transversity angles $\Omega = (\theta_T, \psi_T, \phi_T)$ are defined in section 5.1. The likelihood is independent of the K^+K^- mass distribution. The likelihood function is defined as a combination of the signal and background probability density functions as follows:

$$\begin{aligned}\ln \mathcal{L} = \sum_{i=1}^{N} \{ & w_i \cdot \ln(f_{\rm s} \cdot \mathcal{F}_{\rm s}(m_i, t_i, \sigma_{t_i}, \Omega_i, P(B|Q), p_{{\rm T}_i}) \\ & + f_{\rm s} \cdot f_{B^0} \cdot \mathcal{F}_{B^0}(m_i, t_i, \sigma_{t_i}, \Omega_i, P(B|Q), p_{{\rm T}_i}) \\ & + f_{\rm s} \cdot f_{\Lambda_b} \cdot \mathcal{F}_{\Lambda_b}(m_i, t_i, \sigma_{t_i}, \Omega_i, P(B|Q), p_{{\rm T}_i}) \\ & + (1 - f_{\rm s} \cdot (1 + f_{B^0} + f_{\Lambda_b})) \mathcal{F}_{\rm bkg}(m_i, t_i, \sigma_{t_i}, \Omega_i, P(B|Q), p_{{\rm T}_i}))\}, \end{aligned} \tag{5.1}$$

where N is the number of selected candidates, w_i is a weighting factor to account for the trigger efficiency (described in section 5.3), and $f_{\rm s}$ is the fraction of signal candidates. The background fractions f_{B^0} and f_{Λ_b} are the fractions of B^0 mesons and Λ_b baryons mis-identified as B_s^0 candidates calculated relative to the number of signal events; these parameters are fixed to their MC values and varied as part of the systematic uncertainties. The mass m_i, the proper decay time t_i and the decay angles Ω_i are the values measured from the data for each event i. $\mathcal{F}_{\rm s}$, $\mathcal{F}_{B^0}$, $\mathcal{F}_{\Lambda_b}$ and $\mathcal{F}_{\rm bkg}$ are the probability density functions (PDF) modelling the signal, B^0 background, Λ_b background, and the other background distributions, respectively. A detailed description of the signal PDF terms in equation (5.1) is given in section 5.1. The three background functions are described in section 5.2.

JHEP08(2016)147

5.1 Signal PDF

The PDF used to describe the signal events, $\mathcal{F}_{\rm s}$, has the following composition:

$$\begin{aligned}\mathcal{F}_{\rm s}(m_i, t_i, \sigma_{t_i}, \Omega_i, P(B|Q), p_{{\rm T}_i}) = {} & P_{\rm s}(m_i) \cdot P_{\rm s}(\Omega_i, t_i, P(B|Q), \sigma_{t_i}) \\ & \cdot P_{\rm s}(\sigma_{t_i}) \cdot P_{\rm s}(P(B|Q)) \cdot A(\Omega_i, p_{{\rm T}_i}) \cdot P_{\rm s}(p_{{\rm T}_i}). \end{aligned} \quad (5.2)$$

The mass function $P_{\rm s}(m_i)$ is modelled by a sum of three Gaussian distributions. The probability terms $P_{\rm s}(\sigma_{t_i})$ and $P_{\rm s}(p_{{\rm T}i})$ are described by gamma functions and are unchanged from the analysis described in ref. [25]. The tagging probability term for signal $P_{\rm s}(P(B|Q))$ is described in section 4.3.

The term $P_{\rm s}(\Omega_i, t_i, P(B|Q), \sigma_{t_i})$ is a joint PDF for the decay time t and the transversity angles Ω for the $B_s^0 \to J/\psi(\mu^+\mu^-)\phi(K^+K^-)$ decay. Ignoring detector effects, the distribution for the time t and the angles Ω is given by the differential decay rate [26]:

$$\frac{{\rm d}^4\Gamma}{{\rm dt}\ {\rm d}\Omega} = \sum_{k=1}^{10} \mathcal{O}^{(k)}(t) g^{(k)}(\theta_T, \psi_T, \phi_T),$$

where $\mathcal{O}^{(k)}(t)$ are the time-dependent functions corresponding to the contributions of the four different amplitudes (A_0, $A_{||}$, $A_\perp$, and A_S) and their interference terms, and $g^{(k)}(\theta_T, \psi_T, \phi_T)$ are the angular functions. Table 4 shows these time-dependent functions and the angular functions of the transversity angles. The formulae for the time-dependent functions have the same structure for B_s^0 and $\bar{B}_s^0$ but with a sign reversal in the terms containing Δm_s. In table 4, the parameter $A_\perp(t)$ is the time-dependent amplitude for the CP-odd final-state configuration while $A_0(t)$ and $A_{||}(t)$ correspond to CP-even final-state configurations. The amplitude $A_S(t)$ gives the contribution from the CP-odd non-resonant $B_s^0 \to J/\psi K^+K^-$ S-wave state (which includes the f_0). The corresponding functions are given in the last four lines of table 4 (k = 7–10). The amplitudes are parameterized by $|A_i|e^{i\delta_i}$, where $i = \{0, ||, \perp, S\}$, with $\delta_0 = 0$ and are normalized such that $|A_0(0)|^2 + |A_\perp(0)|^2 + |A_{||}(0)|^2 = 1$. $|A_\perp(0)|$ is determined according to this condition, while the remaining three amplitudes are parameters of the fit. The formalism used throughout this analysis assumes no direct CP violation.

The angles $(\theta_T, \psi_T, \phi_T)$, are defined in the rest frames of the final-state particles. The x-axis is determined by the direction of the ϕ meson in the J/ψ rest frame, and the K^+K^- system defines the x–y plane, where $p_y(K^+) > 0$. The three angles are defined as:

- θ_T, the angle between $\vec{p}(\mu^+)$ and the normal to the x–y plane, in the J/ψ meson rest frame,
- ϕ_T, the angle between the x-axis and $\vec{p}_{xy}(\mu^+)$, the projection of the μ^+ momentum in the x–y plane, in the J/ψ meson rest frame,
- ψ_T, the angle between $\vec{p}(K^+)$ and $-\vec{p}(J/\psi)$ in the ϕ meson rest frame.

The PDF term $P_{\rm s}(\Omega_i, t_i, P(B|Q), \sigma_{t_i})$ takes into account the lifetime resolution, so each time element in table 4 is smeared with a Gaussian function. This smearing is performed

JHEP08(2016)147

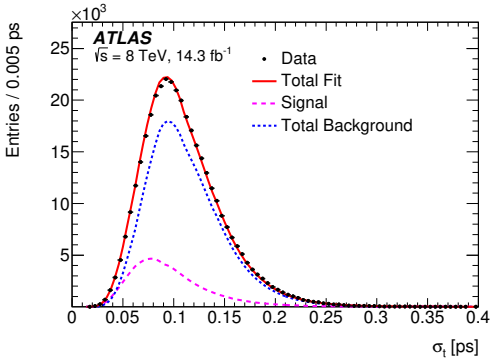

Figure 6. The proper decay time uncertainty distribution for data (black), and the fits to the background (blue) and the signal (purple) contributions. The total fit is shown as a red curve.

numerically on an event-by-event basis where the width of the Gaussian function is the proper decay time uncertainty, measured for each event, multiplied by a scale factor to account for any mis-measurements. The proper decay time uncertainty distribution for data, including the fits to the background and the signal contributions is shown in figure 6. The average value of this uncertainty for signal events is 97 fs.

The angular acceptance of the detector and kinematic cuts on the angular distributions are included in the likelihood function through $A(\Omega_i, p_{Ti})$. This is calculated using a 4D binned acceptance method, applying an event-by-event efficiency according to the transversity angles $(\theta_T, \psi_T, \phi_T)$ and the $p_{\rm T}$ of the candidate. The $p_{\rm T}$ binning is necessary, because the angular acceptance is influenced by the $p_{\rm T}$ of the B_s^0 candidate. The acceptance is calculated from the $B_s^0 \to J/\psi\phi$ MC events. Taking the small discrepancies between data and MC events into account have negligible effect on the fit results. In the likelihood function, the acceptance is treated as an angular acceptance PDF, which is multiplied with the time- and angle-dependent PDF describing the $B_s^0 \to J/\psi(\mu^+\mu^-)\phi(K^+K^-)$ decays. As both the acceptance and time- and angle-dependent decay PDFs depend on the transversity angles they must be normalized together. This normalization is done numerically during the likelihood fit. The PDF is normalized over the entire B_s^0 mass range 5.150–5.650 GeV.

5.2 Background PDF

The background PDF has the following composition:

$$\begin{aligned}\mathcal{F}_{\rm bkg}(m_i, t_i, \sigma_{t_i}, \Omega_i, P(B|Q), p_{{\rm T}_i}) = {} & P_{\rm b}(m_i) \cdot P_{\rm b}(t_i|\sigma_{t_i}) \cdot P_{\rm b}(P(B|Q)) \\ & \cdot P_{\rm b}(\Omega_i) \cdot P_{\rm b}(\sigma_{t_i}) \cdot P_{\rm b}(p_{{\rm T}i}). \end{aligned} \tag{5.3}$$

The proper decay time function $P_{\rm b}(t_i|\sigma_{t_i})$ is parameterized as a prompt peak modelled by a Gaussian distribution, two positive exponential functions and a negative exponential function. These functions are smeared with the same resolution function as the signal decay time-dependence. The prompt peak models the combinatorial background events, which are expected to have reconstructed lifetimes distributed around zero. The two positive exponential functions represent a fraction of longer-lived backgrounds with non-prompt

JHEP08(2016)147

k	$\mathcal{O}^{(k)}(t)$	$g^{(k)}(\theta_T, \psi_T, \phi_T)$
1	$\frac{1}{2}\lvert A_0(0)\rvert^2 \left[(1+\cos\phi_s)\, e^{-\Gamma_{\rm L}^{(s)}t} + (1-\cos\phi_s)\, e^{-\Gamma_{\rm H}^{(s)}t} \pm 2e^{-\Gamma_s t}\sin(\Delta m_s t)\sin\phi_s\right]$	$2\cos^2\psi_T(1-\sin^2\theta_T\cos^2\phi_T)$
2	$\frac{1}{2}\lvert A_\parallel(0)\rvert^2 \left[(1+\cos\phi_s)\, e^{-\Gamma_{\rm L}^{(s)}t} + (1-\cos\phi_s)\, e^{-\Gamma_{\rm H}^{(s)}t} \pm 2e^{-\Gamma_s t}\sin(\Delta m_s t)\sin\phi_s\right]$	$\sin^2\psi_T(1-\sin^2\theta_T\sin^2\phi_T)$
3	$\frac{1}{2}\lvert A_\perp(0)\rvert^2 \left[(1-\cos\phi_s)\, e^{-\Gamma_{\rm L}^{(s)}t} + (1+\cos\phi_s)\, e^{-\Gamma_{\rm H}^{(s)}t} \mp 2e^{-\Gamma_s t}\sin(\Delta m_s t)\sin\phi_s\right]$	$\sin^2\psi_T\sin^2\theta_T$
4	$\frac{1}{2}\lvert A_0(0)\rvert\lvert A_\parallel(0)\rvert\cos\delta_\parallel$ $\left[(1+\cos\phi_s)\, e^{-\Gamma_{\rm L}^{(s)}t} + (1-\cos\phi_s)\, e^{-\Gamma_{\rm H}^{(s)}t} \pm 2e^{-\Gamma_s t}\sin(\Delta m_s t)\sin\phi_s\right]$	$\frac{1}{\sqrt{2}}\sin 2\psi_T\sin^2\theta_T\sin 2\phi_T$
5	$\lvert A_\parallel(0)\rvert\lvert A_\perp(0)\rvert[\frac{1}{2}(e^{-\Gamma_{\rm L}^{(s)}t} - e^{-\Gamma_{\rm H}^{(s)}t})\cos(\delta_\perp-\delta_\parallel)\sin\phi_s$ $\pm e^{-\Gamma_s t}(\sin(\delta_\perp-\delta_\parallel)\cos(\Delta m_s t) - \cos(\delta_\perp-\delta_\parallel)\cos\phi_s\sin(\Delta m_s t))]$	$-\sin^2\psi_T\sin 2\theta_T\sin\phi_T$
6	$\lvert A_0(0)\rvert\lvert A_\perp(0)\rvert[\frac{1}{2}(e^{-\Gamma_{\rm L}^{(s)}t} - e^{-\Gamma_{\rm H}^{(s)}t})\cos\delta_\perp\sin\phi_s$ $\pm e^{-\Gamma_s t}(\sin\delta_\perp\cos(\Delta m_s t) - \cos\delta_\perp\cos\phi_s\sin(\Delta m_s t))]$	$\frac{1}{\sqrt{2}}\sin 2\psi_T\sin 2\theta_T\cos\phi_T$
7	$\frac{1}{2}\lvert A_S(0)\rvert^2 \left[(1-\cos\phi_s)\, e^{-\Gamma_{\rm L}^{(s)}t} + (1+\cos\phi_s)\, e^{-\Gamma_{\rm H}^{(s)}t} \mp 2e^{-\Gamma_s t}\sin(\Delta m_s t)\sin\phi_s\right]$	$\frac{2}{3}\left(1-\sin^2\theta_T\cos^2\phi_T\right)$
8	$\lvert A_S(0)\rvert\lvert A_\parallel(0)\rvert[\frac{1}{2}(e^{-\Gamma_{\rm L}^{(s)}t} - e^{-\Gamma_{\rm H}^{(s)}t})\sin(\delta_\parallel-\delta_S)\sin\phi_s$ $\pm e^{-\Gamma_s t}(\cos(\delta_\parallel-\delta_S)\cos(\Delta m_s t) - \sin(\delta_\parallel-\delta_S)\cos\phi_s\sin(\Delta m_s t))]$	$\frac{1}{3}\sqrt{6}\sin\psi_T\sin^2\theta_T\sin 2\phi_T$
9	$\frac{1}{2}\lvert A_S(0)\rvert\lvert A_\perp(0)\rvert\sin(\delta_\perp-\delta_S)$ $\left[(1-\cos\phi_s)\, e^{-\Gamma_{\rm L}^{(s)}t} + (1+\cos\phi_s)\, e^{-\Gamma_{\rm H}^{(s)}t} \mp 2e^{-\Gamma_s t}\sin(\Delta m_s t)\sin\phi_s\right]$	$\frac{1}{3}\sqrt{6}\sin\psi_T\sin 2\theta_T\cos\phi_T$
10	$\lvert A_0(0)\rvert\lvert A_S(0)\rvert[\frac{1}{2}(e^{-\Gamma_{\rm H}^{(s)}t} - e^{-\Gamma_{\rm L}^{(s)}t})\sin\delta_S\sin\phi_s$ $\pm e^{-\Gamma_s t}(\cos\delta_S\cos(\Delta m_s t) + \sin\delta_S\cos\phi_s\sin(\Delta m_s t))]$	$\frac{4}{3}\sqrt{3}\cos\psi_T\left(1-\sin^2\theta_T\cos^2\phi_T\right)$

Table 4. Table showing the ten time-dependent functions, $\mathcal{O}^{(k)}(t)$ and the functions of the transversity angles $g^{(k)}(\theta_T, \psi_T, \phi_T)$. The amplitudes $|A_0(0)|^2$ and $|A_\parallel(0)|^2$ are for the CP-even components of the $B_s^0 \to J/\psi\phi$ decay, $|A_\perp(0)|^2$ is the CP-odd amplitude; they have corresponding strong phases δ_0, $\delta_\parallel$ and $\delta_\perp$. By convention δ_0 is set to be zero. The S-wave amplitude $|A_S(0)|^2$ gives the fraction of $B_s^0 \to J/\psi K^+K^-(f_0)$ and has a related strong phase δ_S. The $\pm$ and $\mp$ terms denote two cases: the upper sign describes the decay of a meson that was initially a B_s^0 meson, while the lower sign describes the decays of a meson that was initially $\bar{B}_s^0$.

J/ψ, combined with hadrons from the primary vertex or from a B/D meson in the same event. The negative exponential function takes into account events with poor vertex resolution. The probability terms $P_{\rm b}(\sigma_{t_i})$ and $P_{\rm b}(p_{{\rm T}i})$ are described by gamma functions. They are unchanged from the analysis described in ref. [25] and explained in detail there. The tagging probability term for background $P_{\rm b}(P(B|Q))$ is described in section 4.3.

The shape of the background angular distribution, $P_{\rm b}(\Omega_i)$ arises primarily from detector and kinematic acceptance effects. These are described by Legendre polynomial functions:

$$
\begin{aligned}
Y_l^m(\theta_T) &= \sqrt{(2l+1)/(4\pi)}\sqrt{(l-m)!/(l+m)!}P_l^{|m|}(\cos\theta_T) \\
P_k(x) &= \frac{1}{2^k k!}\frac{{\rm d}^{\rm k}}{{\rm dx}^{\rm k}}(x^2-1)^k \qquad (5.4)\\
\mathscr{P}_{\rm b}(\theta_T,\psi_T,\phi_T) &= \sum_{k=0}^{6}\sum_{l=0}^{6}\sum_{m=-l}^{l}\begin{cases} a_{k,l,m}\sqrt{2}Y_l^m(\theta_T)\cos(m\phi_T)P_k(\cos\psi_T) & \text{where } m>0 \\ a_{k,l,m}\sqrt{2}Y_l^{-m}(\theta_T)\sin(m\phi_T)P_k(\cos\psi_T) & \text{where } m<0 \\ a_{k,l,m}\sqrt{2}Y_l^0(\theta_T)P_k(\cos\psi_T) & \text{where } m=0 \end{cases}
\end{aligned}
$$

where the coefficients $a_{k,l,m}$ are adjusted to give the best fit to the angular distributions for events in the B_s^0 mass sidebands. These parameters are then fixed in the main fit. The B_s^0 mass interval used for the background fit is between 5.150 and 5.650 GeV excluding the signal mass region $|(m(B_s^0) - 5.366\ \text{GeV}| < 0.110$ GeV. The background mass model, $P_{\rm b}(m_i)$ is an exponential function with a constant term added.

Contamination from $B_d \to J/\psi K^{0*}$ and $\Lambda_b \to J/\psi p K^-$ events mis-reconstructed as $B_s^0 \to J/\psi\phi$ are accounted for in the fit through the $\mathcal{F}_{B^0}$ and $\mathcal{F}_{\Lambda_b}$ terms in the PDF function described in equation (5.1). The fraction of these contributions, $f_{B^0} = (3.3 \pm 0.5)\%$ and $f_{\Lambda_b} = (1.8 \pm 0.6)\%$, are evaluated from MC simulation using production and branching fractions from refs. [18, 27–31]. MC simulated events are also used to determine the shape of the mass and transversity angle distributions. The 3D angular distributions of $B_d^0 \to J/\psi K^{*0}$ and of the conjugate decay are modelled using input from ref. [32], while angular distributions for $\Lambda_b \to J/\psi p K^-$ and the conjugate decay are modelled as flat. These distributions are sculpted for detector acceptance effects and then described by Legendre polynomial functions, equation (5.4), as in the case of the background described by equation (5.3). These shapes are fixed in the fit. The B_d and Λ_b lifetimes are accounted for in the fit by adding additional exponential terms, scaled by the ratio of B_d/B_s^0 or Λ_b/B_s^0 masses as appropriate, where the lifetimes and masses are taken from ref. [18]. Systematic uncertainties due to the background from $B_d \to J/\psi K^{0*}$ and $\Lambda_b \to J/\psi p K^-$ decays are described in section 7. The contribution of $B_d \to J/\psi K\pi$ events as well as their interference with $B_d \to J/\psi K^{0*}$ events is not included in the fit and is instead assigned as a systematic uncertainty.

To account for possible deviations between data and the selected fit models a number of alternative fit functions and mass selection criteria are used to determine systematic uncertainties in the B_s^0 fit. These fit variations are described in section 7.

JHEP08(2016)147

5.3 Muon trigger proper time-dependent efficiency

It was observed that the muon trigger biases the transverse impact parameter of muons, resulting in a minor inefficiency at large values of the proper decay time. This inefficiency is measured using MC simulated events, by comparing the B_s^0 proper decay time distribution of an unbiased sample with the distribution obtained including the trigger. To account for this inefficiency in the fit, the events are re-weighted by a factor w:

$$w = p_0 \cdot [1 - p_1 \cdot (\mathrm{Erf}((\mathrm{t} - \mathrm{p_3})/\mathrm{p_2}) + 1)], \tag{5.5}$$

where p_0, p_1, p_2 and p_3 are parameters determined in the fit to MC events. No significant bias or inefficiency due to off-line track reconstruction, vertex reconstruction, or track quality selection criteria is observed.

6 Results

The full simultaneous unbinned maximum-likelihood fit contains nine physical parameters: $\Delta\Gamma_s$, ϕ_s, Γ_s, $|A_0(0)|^2$, $|A_\parallel(0)|^2$, $\delta_\parallel$, $\delta_\perp$, $|A_S(0)|^2$ and δ_S. The other parameters in the likelihood function are the B_s^0 signal fraction f_s, parameters describing the $J/\psi\phi$ mass distribution, parameters describing the B_s^0 meson decay time plus angular distributions of background events, parameters used to describe the estimated decay time uncertainty distributions for signal and background events, and scale factors between the estimated decay time uncertainties and their true uncertainties. In addition there are also 353 nuisance parameters describing the background and acceptance functions that are fixed at the time of the fit. The fit model is tested using pseudo-experiments as described in section 7. These tests show no significant bias, as well as no systematic underestimation of the statistical errors reported from the fit to data.

Multiplying the total number of events supplied to the fit with the extracted signal fraction and its statistical uncertainty provides an estimate for the total number of B_s^0 meson candidates of 74900 ± 400. The results and correlations of the physics parameters obtained from the fit are given in tables 5 and 6. Fit projections of the mass, proper decay time and angles are given in figures 7 and 8, respectively.

7 Systematic uncertainties

Systematic uncertainties are assigned by considering effects that are not accounted for in the likelihood fit. These are described below.

- **Flavour tagging:** there are two contributions to the uncertainties in the fit parameters due to the flavour tagging procedure, the statistical and systematic components. The statistical uncertainty due to the size of the sample of $B^\pm \to J/\psi K^\pm$ decays is included in the overall statistical error. The systematic uncertainty arising from the precision of the tagging calibration is estimated by changing the model used to parameterize the probability distribution, $P(B|Q)$, as a function of tag charge from the third-order polynomial function used by default to one of several alternative

JHEP08(2016)147

Parameter	Value	Statistical uncertainty	Systematic uncertainty
ϕ_s[rad]	-0.110	0.082	0.042
$\Delta\Gamma_s$[ps^{-1}]	0.101	0.013	0.007
Γ_s[ps^{-1}]	0.676	0.004	0.004
$\lvert A_{\parallel}(0)\rvert^2$	0.230	0.005	0.006
$\lvert A_0(0)\rvert^2$	0.520	0.004	0.007
$\lvert A_S(0)\rvert^2$	0.097	0.008	0.022
$\delta_\perp$ [rad]	4.50	0.45	0.30
$\delta_{\parallel}$ [rad]	3.15	0.10	0.05
$\delta_\perp - \delta_S$ [rad]	-0.08	0.03	0.01

Table 5. Fitted values for the physical parameters of interest with their statistical and systematic uncertainties.

	$\Delta\Gamma$	Γ_s	$\lvert A_{\parallel}(0)\rvert^2$	$\lvert A_0(0)\rvert^2$	$\lvert A_S(0)\rvert^2$	$\delta_{\parallel}$	$\delta_\perp$	$\delta_\perp - \delta_S$
ϕ_s	0.097	-0.085	0.030	0.029	0.048	0.067	0.035	-0.008
$\Delta\Gamma$	1	-0.414	0.098	0.136	0.045	0.009	0.008	-0.011
Γ_s		1	-0.119	-0.042	0.167	-0.027	-0.009	0.018
$\lvert A_{\parallel}(0)\rvert^2$			1	-0.330	0.072	0.105	0.025	-0.018
$\lvert A_0(0)\rvert^2$				1	0.234	-0.011	0.007	0.014
$\lvert A_S(0)\rvert^2$					1	-0.046	0.004	0.052
$\delta_{\parallel}$						1	0.158	-0.006
$\delta_\perp$							1	0.018

Table 6. Fit correlations between the physical parameters of interest.

functions. The alternatives used are: a linear function; a fifth-order polynomial; or two third-order polynomials describing the positive and negative regions that share the constant and linear terms but have independent quadratic and cubic terms. For the combined-muon tagging, an additional model consisting of two third-order polynomials sharing the constant term but with independent linear, quadratic and cubic terms is also used. The B_s^0 fit is repeated using the alternative models and the largest difference is assigned as the systematic uncertainty.

- **Angular acceptance method:** the angular acceptance (from the detector and kinematic effects mentioned in section 5.1) is calculated from a binned fit to MC simulated data. In order to estimate the size of the systematic uncertainty introduced from the choice of binning, different acceptance functions are calculated using different bin widths and central values. These effects are found to be negligible.

JHEP08(2016)147

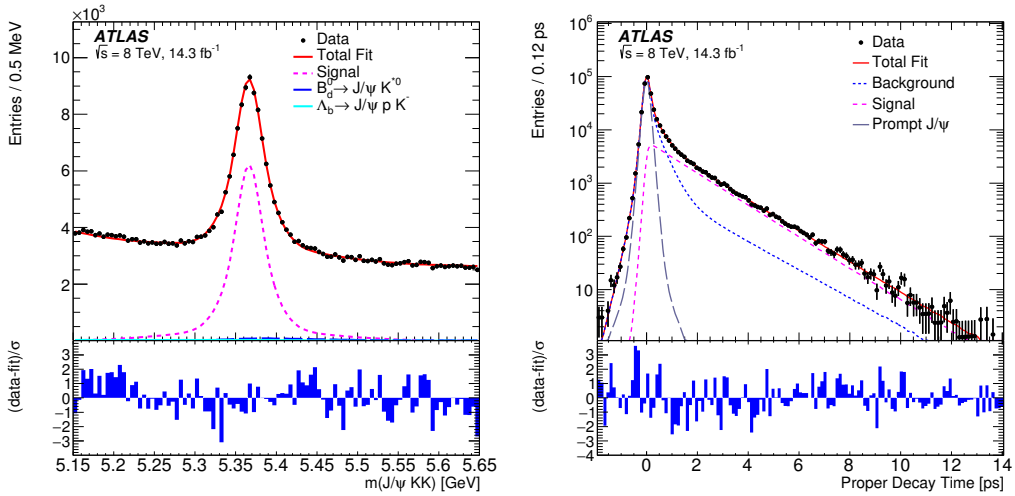

Figure 7. (Left) Mass fit projection for the $B_s^0 \to J/\psi\phi$ sample. The red line shows the total fit, the dashed purple line shows the signal component, the long-dashed dark blue line shows the $B_d^0 \to J/\psi K^{0*}$ component, while the solid light blue line shows the contribution from $\Lambda_b \to J/\psi p K^-$ events. (Right) Proper decay time fit projection for the $B_s^0 \to J/\psi\phi$ sample. The red line shows the total fit while the purple dashed line shows the total signal. The total background is shown as a blue dashed line with a long-dashed grey line showing the prompt J/ψ background. Below each figure is a ratio plot that shows the difference between each data point and the total fit line divided by the statistical uncertainty (σ) of that point.

- **Inner detector alignment:** residual misalignments of the ID affect the impact parameter, d_0, distribution with respect to the primary vertex. The effect of a radial expansion on the measured d_0 is determined from data collected at 8 TeV, with a trigger requirement of at least one muon with a transverse momentum greater than or equal to 4 GeV. The radial expansion uncertainties determined in this way are 0.14% for $|\eta| < 1.5$ and 0.55% for $1.5 < |\eta| < 2.5$. These values are used to estimate the effect on the fitted B_s^0 parameter values. Small deviations are seen in some parameters, and these are included as systematic uncertainties.

- **Trigger efficiency:** to correct for the trigger lifetime bias the events are re-weighted according to equation (5.5). The uncertainty of the parameters p_0, p_1, p_2 and p_3 are used to estimate the systematic uncertainty due to the time efficiency correction. These uncertainties originate from the following sources: the limited size of the MC simulated dataset, the choice of bin-size for the proper decay time distributions and variations between different triggers. The systematic effects are found to be negligible.

- **Background angles model, choice of p_{T} bins:** the shape of the background angular distribution, $P_{\mathrm{b}}(\theta_T, \varphi_T, \psi_T)$, is described by the Legendre polynomial functions given in equation (5.4). The shapes arise primarily from detector and kinematic acceptance effects and are sensitive to the p_{T} of the B_s^0 meson candidate. For this reason, the parameterization using the Legendre polynomial functions is performed in four p_{T} intervals: 0–13 GeV, 13–18 GeV, 18–25 GeV and >25 GeV. The system-

JHEP08(2016)147

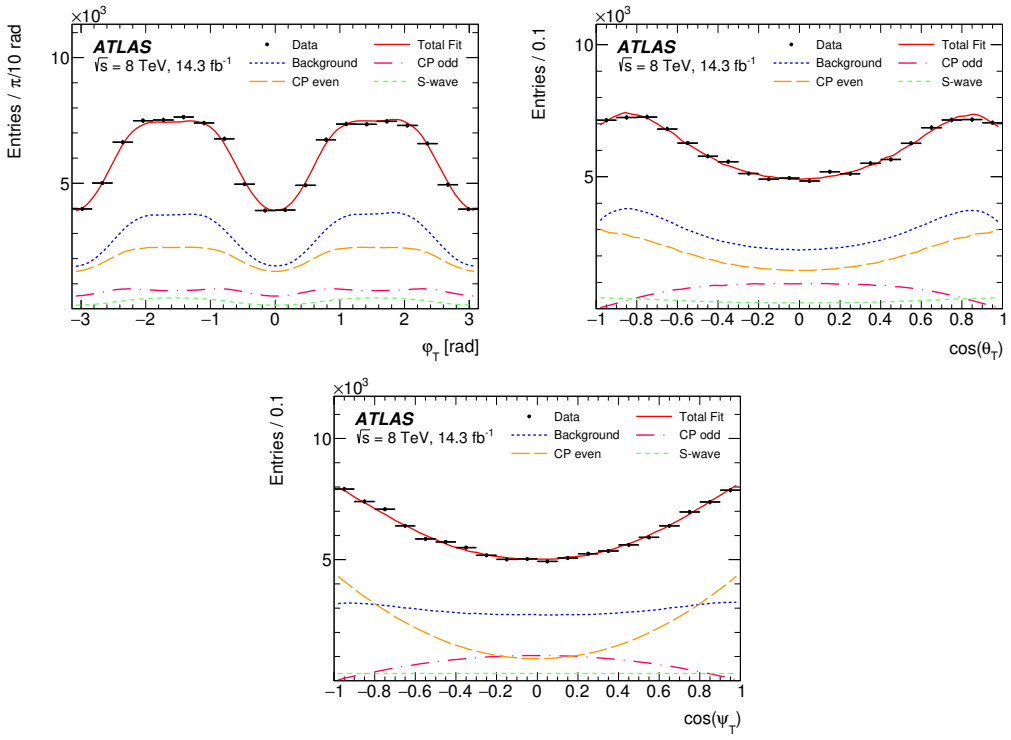

Figure 8. Fit projections for the transversity angles of events with 5.317 GeV $< m(J/\psi KK) <$ 5.417 GeV for ϕ_T (top left), $\cos(\theta_T)$ (top right), and $\cos(\psi_T)$ (bottom). In all three plots the red solid line shows the total fit, the CP-odd and CP-even signal components are shown by the red dot-dashed and orange dashed lines respectively, the S-wave component is given by the green dashed line and the blue dotted line shows the background contribution. The contributions of the interference terms are negligible in these projections and are not shown.

atic uncertainties due to the choice of $p_{\rm T}$ intervals are estimated by repeating the fit, varying these intervals. The biggest deviations observed in the fit results were taken to represent the systematic uncertainties.

- **Background angles model, choice of mass sidebands:** the parameters of the Legendre polynomial functions given in equation (5.4) are adjusted to give the best fit to the angular distributions for events in the B_s^0 mass sidebands. To test the sensitivity of the fit results to the choice of sideband regions, the fit is repeated with alternative choices for the excluded signal mass regions: $|m(B_s^0) - 5.366| > 0.085$ GeV and $|m(B_s^0) - 5.366| > 0.160$ GeV (instead of $|m(B_s^0) - 5.366| > 0.110$ GeV). The differences in the fit results are assigned as systematic uncertainties.

- ***B_d* contribution:** the contamination from $B_d \to J/\psi K^{0*}$ events mis-reconstructed as $B_s^0 \to J/\psi\phi$ is accounted for in the final fit. Studies are performed to evaluate the effect of the uncertainties in the $B_d \to J/\psi K^{0*}$ fraction, and the shapes of the mass and transversity angles distribution. In the MC events the angular distribution of the $B_d \to J/\psi K^{0*}$ decay is modelled using parameters taken from ref. [32]. The uncertainties of these parameters are taken into account in the estimation of systematic

JHEP08(2016)147

uncertainty. After applying the B_s^0 signal selection cuts, the angular distributions are fitted using Legendre polynomial functions. The uncertainties of this fit are included in the systematic tests. The impact of all these uncertainties is found to have a negligible effect on the B_s^0 fit results. The contribution of $B_d \to J/\psi K\pi$ events as well as their interference with $B_d \to J/\psi K^{0*}$ events is not included in the fit and is instead assigned as a systematic uncertainty. To evaluate this uncertainty, the MC background events are modelled using both the P-wave $B_d \to J/\psi K^{0*}$ and S-wave $B_d \to J/\psi K\pi$ decays and their interference, using the input parameters taken from ref. [32]. The B_s^0 fit using this input was compared to the default fit, and differences are included in table 7.

- **Λ_b contribution:** the contamination from $\Lambda_b \to J/\psi p K^-$ events mis-reconstructed as $B_s^0 \to J/\psi\phi$ is accounted for in the final fit. Studies are performed to evaluate the effect of the uncertainties in the $\Lambda_b \to J/\psi p K^-$ fraction f_{Λ_b}, and the shapes of the mass, transversity angles, and lifetime distributions. Additional studies are performed to determine the effect of the uncertainties in the $\Lambda_b \to J/\psi\Lambda^*$ branching ratios used to reweight the generated MC. These are uncertainties are included in table 7.

- **Fit model variations:** to estimate the systematic uncertainties due to the fit model, variations of the model are tested in pseudo-experiments. A set of ≈2500 pseudo-experiments is generated for each variation considered, and fitted with the default model. The systematic error quoted for each effect is the difference between the mean shift of the fitted value of each parameter from its input value for the pseudo-experiments altered for each source of systematic uncertainty. In the first variation tested, the signal mass is generated using the fitted B_s^0 mass convolved with a Gaussian function using the measured per-candidate mass errors. In another test, the background mass is generated from an exponential function with the addition of a first-degree polynomial function instead of an exponential function plus a constant term. The time resolution model was varied by using two different scale factors to generate the lifetime uncertainty, instead of the single scale factor used in the default model. The non-negligible uncertainties derived from these tests are included in the systematic uncertainties shown in table 7. To determine the possible systematics effects of mis-modelling of the background events by the fitted background model, as seen in the low mass side-band region (5.150–5.210 GeV) of figure 7, left, alternative mass selection cuts are used with the default fit model. The effect of these changes on the fit results are found to be negligible.

- **Default fit model:** due to its complexity, the fit model is less sensitive to some nuisance parameters. This limited sensitivity could potentially lead to a bias in the measured physics parameters, even when the model perfectly describes the fitted data. To estimate the systematic uncertainty due to the choice of default fit model, a set of pseudo-experiments were conducted using the default model in both the generation and fit. The systematic uncertainties are determined from the mean of

JHEP08(2016)147

	ϕ_s [rad]	$\Delta\Gamma_s$ [ps^{-1}]	Γ_s [ps^{-1}]	$\lvert A_\parallel(0)\rvert^2$	$\lvert A_0(0)\rvert^2$	$\lvert A_S(0)\rvert^2$	$\delta_\perp$ [rad]	$\delta_\parallel$ [rad]	$\delta_\perp - \delta_S$ [rad]
Tagging	0.025	0.003	$<10^{-3}$	$<10^{-3}$	$<10^{-3}$	0.001	0.236	0.014	0.004
Acceptance	$<10^{-3}$	$<10^{-3}$	$<10^{-3}$	0.003	$<10^{-3}$	0.001	0.004	0.008	$<10^{-3}$
Inner detector alignment	0.005	$<10^{-3}$	0.002	$<10^{-3}$	$<10^{-3}$	$<10^{-3}$	0.134	0.007	$<10^{-3}$
Background angles model:									
Choice of p_{T} bins	0.020	0.006	0.003	0.003	$<10^{-3}$	0.008	0.004	0.006	0.008
Choice of mass interval	0.008	0.001	0.001	$<10^{-3}$	$<10^{-3}$	0.002	0.021	0.005	0.003
B_d^0 background model	0.023	0.001	$<10^{-3}$	0.002	0.002	0.017	0.090	0.011	0.009
Λ_b background model	0.011	0.002	0.001	0.001	0.007	0.009	0.045	0.006	0.007
Fit model:									
Mass signal model	0.004	$<10^{-3}$	$<10^{-3}$	0.002	$<10^{-3}$	0.001	0.015	0.017	$<10^{-3}$
Mass background model	$<10^{-3}$	0.002	$<10^{-3}$	0.002	$<10^{-3}$	0.002	0.027	0.038	$<10^{-3}$
Time resolution model	0.003	$<10^{-3}$	0.001	0.002	$<10^{-3}$	0.002	0.057	0.011	0.001
Default fit model	0.001	0.002	$<10^{-3}$	0.002	$<10^{-3}$	0.002	0.025	0.015	0.002
Total	0.042	0.007	0.004	0.006	0.007	0.022	0.30	0.05	0.01

Table 7. Summary of systematic uncertainties assigned to the physical parameters of interest.

the pull distributions of the pseudo-experiments scaled by the statistical error of that parameter on the fit to data. These tests show no significant bias in the fit model, and no systematic underestimation of the statistical errors reported from the fit to data.

The systematic uncertainties are listed in table 7. For each parameter, the total systematic error is obtained by adding all of the contributions in quadrature.

8 Discussion

The PDF describing the $B_s^0 \to J/\psi\phi$ decay is invariant under the following simultaneous transformations:

$$\{\phi_s, \Delta\Gamma_s, \delta_\perp, \delta_\parallel\} \to \{\pi - \phi_s, -\Delta\Gamma_s, \pi - \delta_\perp, 2\pi - \delta_\parallel\}.$$

Since $\Delta\Gamma_s$ was determined to be positive [33], there is a unique solution. Figure 9 shows the 1D log-likelihood scans of ϕ_s, $\Delta\Gamma_s$ and of the three measured strong phases $\delta_{||}$, $\delta_\perp$ and $\delta_\perp - \delta_S$. The variable on vertical axis, $2\Delta\ln(\mathrm{L}) \equiv 2(\ln(\mathrm{L^G}) - \ln(\mathrm{L^i}))$, is a difference between the likelihood values of a default fit, $(\mathrm{L^G})$, and of the fit in which the physical parameter is fixed to a value shown on horizontal axis, $(\mathrm{L^i})$. $2\Delta\ln(\mathrm{L}) = 1$ corresponds to the estimated 1σ confidence level. There are a small asymmetries in the likelihood curves, however at the level of one statistical σ these are small compared to the corresponding statistical uncertainties of the physical variables, for which the scan is done. Therefore symmetric statistical uncertainties are quoted. Figure 10 shows the likelihood contours in the ϕ_s–$\Delta\Gamma_s$ plane. The region predicted by the Standard Model is also shown.

JHEP08(2016)147

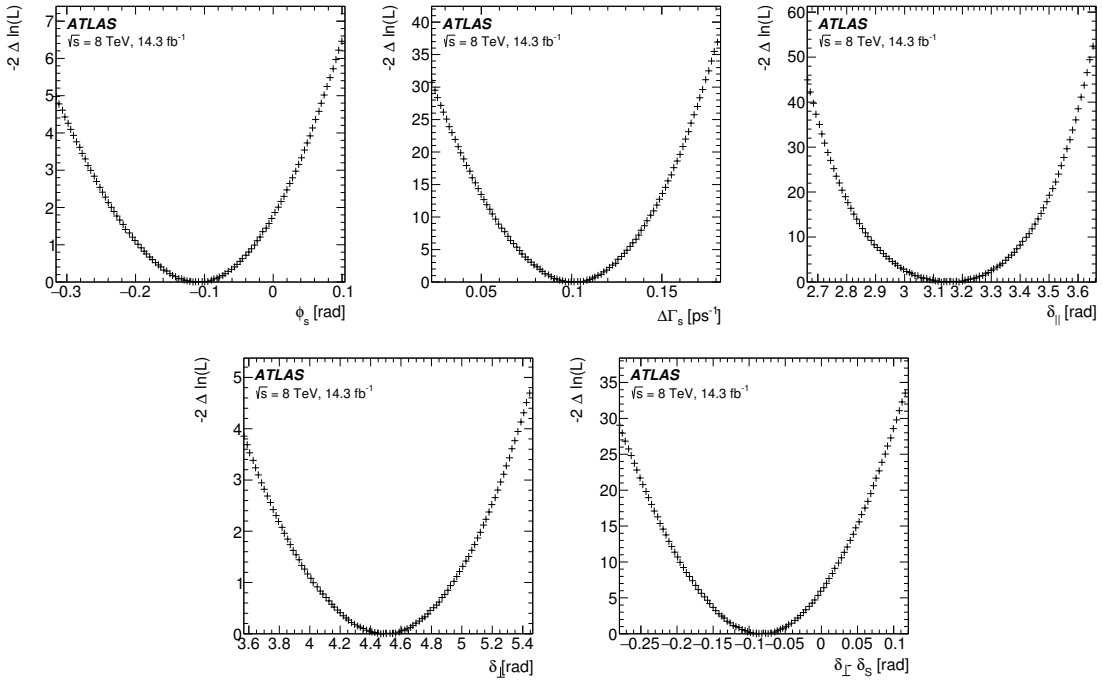

Figure 9. 1D likelihood contours (statistical errors only) for ϕ_s (top left), $\Delta\Gamma_s$ (top centre), $\delta_{||}$ (top right), $\delta_\perp$ (bottom left) and $\delta_\perp - \delta_S$ (bottom right).

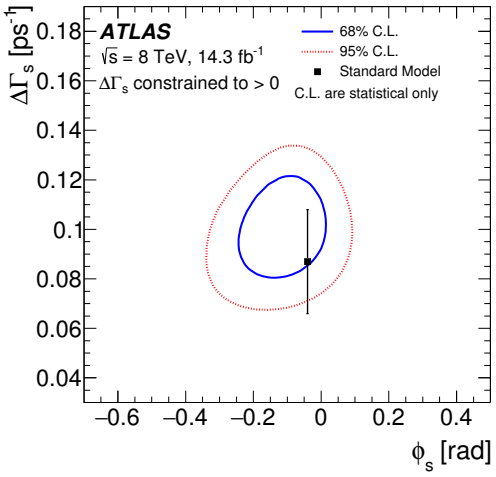

Figure 10. Likelihood contours in the ϕ_s–$\Delta\Gamma_s$ plane for 8 TeV data. The blue line shows the 68% likelihood contour, while the red dotted line shows the 95% likelihood contour (statistical errors only). The SM prediction is taken from ref. [1], at this scale the uncertainty on ϕ_s is not visible on the figure.

JHEP08(2016)147

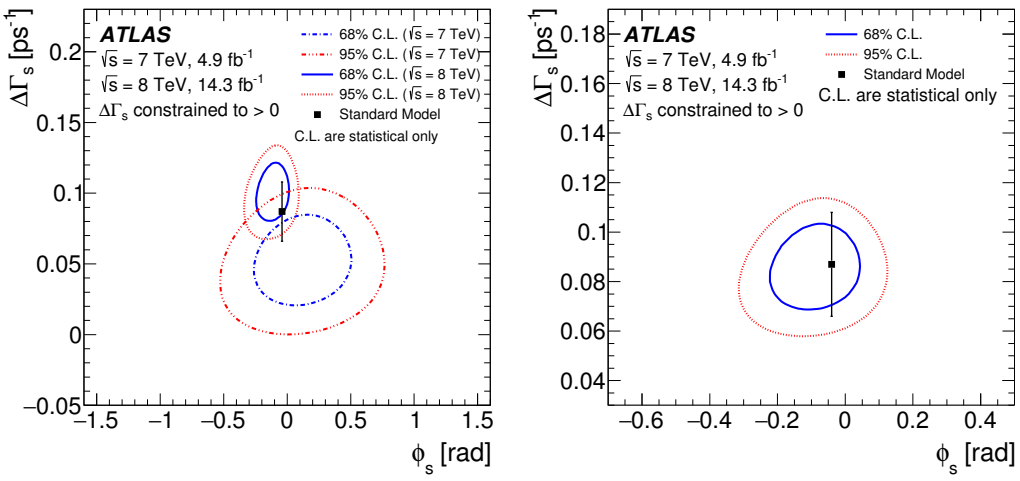

Figure 11. Likelihood contours in the ϕ_s–$\Delta\Gamma_s$ plane for individual results from 7 TeV and 8 TeV data (left) and a final statistical combination of the results from 7 TeV and 8 TeV data (right). The blue line shows the 68% likelihood contour, while the red dotted line shows the 95% likelihood contour (statistical errors only). The SM prediction is taken from ref. [1], at this scale the uncertainty on ϕ_s is not visible on the figure.

9 Combination of 7 TeV and 8 TeV results

The measured values are consistent with those obtained in a previous analysis [8], using ATLAS data collected in 2011 at a centre-of-mass energy of 7 TeV. This consistency is also clear from a comparison of the likelihood contours in the ϕ_s–$\Delta\Gamma_s$ projection shown in figure 11. A Best Linear Unbiased Estimate (BLUE) combination [34] is used to combine the 7 TeV and 8 TeV measurements to give an overall result for Run 1. In ref. [8] the strong phases $\delta_{\parallel}$ and $\delta_{\perp}$–δ_S were given as 1σ confidence intervals. These are not considered in the combination and the 8 TeV result is taken as the Run 1 result.

The BLUE combination requires the measured values and uncertainties of the parameters in question as well as the correlations between them. These are provided by the fits separately in the 7 TeV and 8 TeV measurements. The statistical correlation between these two measurements is zero as the events are different. The correlations of the systematic uncertainties between the two measurements are estimated by splitting the uncertainty into several categories.

The trigger efficiency is included as a systematic uncertainty only in the 7 TeV measurement, so there is no correlation with the 8 TeV measurement. Similarly, the systematic uncertainties arising from the $\Lambda_b \to J/\psi p K^-$ background, and the choice of p_{T} bins and mass sidebands in the modelling of background angles, are included as systematic uncertainties only in the 8 TeV measurement so there is no correlation with the 7 TeV measurement. In both the 7 TeV and 8 TeV results, a systematic uncertainty is assigned to the inner detector alignment and B_d contribution. The inner detector alignment systematic uncertainties are highly correlated and small. The assumed correlation between these systematics made no difference to the final combined result and was set to 100%. For the B_d

JHEP08(2016)147

	8 TeV data			7 TeV data			Run1 combined		
Par	Value	Stat	Syst	Value	Stat	Syst	Value	Stat	Syst
ϕ_s[rad]	-0.110	0.082	0.042	0.12	0.25	0.05	-0.090	0.078	0.041
$\Delta\Gamma_s[\mathrm{ps}^{-1}]$	0.101	0.013	0.007	0.053	0.021	0.010	0.085	0.011	0.007
$\Gamma_s[\mathrm{ps}^{-1}]$	0.676	0.004	0.004	0.677	0.007	0.004	0.675	0.003	0.003
$\lvert A_\parallel(0)\rvert^2$	0.230	0.005	0.006	0.220	0.008	0.009	0.227	0.004	0.006
$\lvert A_0(0)\rvert^2$	0.520	0.004	0.007	0.529	0.006	0.012	0.522	0.003	0.007
$\lvert A_S\rvert^2$	0.097	0.008	0.022	0.024	0.014	0.028	0.072	0.007	0.018
$\delta_\perp$ [rad]	4.50	0.45	0.30	3.89	0.47	0.11	4.15	0.32	0.16
$\delta_\parallel$ [rad]	3.15	0.10	0.05	[3.04, 3.23]		0.09	3.15	0.10	0.05
$\delta_\perp - \delta_S$ [rad]	-0.08	0.03	0.01	[3.02, 3.25]		0.04	-0.08	0.03	0.01

Table 8. Current measurement using data from 8 TeV pp collisions, the previous measurement using data taken at centre of mass energy of 7 TeV and the values for the parameters of the two measurements, statistically combined.

contribution, while the systematic uncertainty tests are different, they are both performed to account for an imprecise knowledge of the B_d contribution and are therefore assumed to be 100%. The tagging, acceptance and fit model uncertainties are quoted for both 7 TeV and 8 TeV. For the fit model, there are several different model variations each with their own uncertainty. For each year, these are summed in quadrature to produce a single fit model systematic uncertainty.

The tagging, acceptance and fit model systematic uncertainties are each assigned a variable (ρ_i, where $i = \mathrm{tag}, \mathrm{acc}, \mathrm{mod}$) corresponding to the correlation between the 7 TeV and 8 TeV results. Several different combinations were tried with different values of $\rho_i = 0, 0.25, 0.5, 0.75, 1.0$. The acceptance systematic uncertainty is small and therefore regardless of what value of ρ_{acc} is chosen the combination stays the same. For the 8 TeV measurement, electron tagging is added, therefore the systematic uncertainty is not 100% correlated. For $\rho_{\mathrm{tag}} = 0.25, 0.5, 0.75$ there is negligible difference between the results. The fit model was changed between the 7 TeV and 8 TeV measurement, the most significant change is that the mass uncertainty modelling was removed and the event-by-event Gaussian error distribution was replaced with a sum of three Gaussian distributions. It would be incorrect to estimate the correlation as 100% and there is negligible difference between the results for $\rho_{\mathrm{mod}} = 0.25, 0.5, 0.75$.

The combined results for the fit parameters and their uncertainties for Run 1 are given in table 8. Due to the negative correlation between Γ_s and $\Delta\Gamma_s$, and the change in the value of $\Delta\Gamma_s$ between the 7 TeV and 8 TeV results, the combined value of Γ_s is less than either individual result. The Run 1 likelihood contours in the ϕ_s–$\Delta\Gamma_s$ plane are shown in figure 11. They agree with the Standard Model predictions.

JHEP08(2016)147

10 Summary

A measurement of the time-dependent CP asymmetry parameters in $B_s^0 \to J/\psi(\mu^+\mu^-)\phi(K^+K^-)$ decays from a 14.3 fb^{-1} data sample of pp collisions collected with the ATLAS detector during the 8 TeV LHC run is presented. The values from the 8 TeV analysis are consistent with those obtained in the previous analysis using 7 TeV ATLAS data [8]. The two measurements are statistically combined leading to the following results:

$$\begin{aligned}
\phi_s &= -0.090 \pm 0.078\ (\text{stat.}) \pm 0.041\ (\text{syst.})\ \text{rad} \\
\Delta\Gamma_s &= 0.085 \pm 0.011\ (\text{stat.}) \pm 0.007\ (\text{syst.})\ \text{ps}^{-1} \\
\Gamma_s &= 0.675 \pm 0.003\ (\text{stat.}) \pm 0.003\ (\text{syst.})\ \text{ps}^{-1} \\
|A_\parallel(0)|^2 &= 0.227 \pm 0.004\ (\text{stat.}) \pm 0.006\ (\text{syst.}) \\
|A_0(0)|^2 &= 0.522 \pm 0.003\ (\text{stat.}) \pm 0.007\ (\text{syst.}) \\
|A_S(0)|^2 &= 0.072 \pm 0.007\ (\text{stat.}) \pm 0.018\ (\text{syst.}) \\
\delta_\perp &= 4.15 \pm 0.32\ (\text{stat.}) \pm\ 0.16\ (\text{syst.})\ \text{rad} \\
\delta_\parallel &= 3.15 \pm 0.10\ (\text{stat.}) \pm\ 0.05\ (\text{syst.})\ \text{rad} \\
\delta_\perp - \delta_S &= -0.08 \pm 0.03\ (\text{stat.}) \pm 0.01\ (\text{syst.})\ \text{rad}.
\end{aligned}$$

The ATLAS Run 1 results for the $B_s^0 \to J/\psi\phi$ decay are consistent with the SM.

Acknowledgments

We thank CERN for the very successful operation of the LHC, as well as the support staff from our institutions without whom ATLAS could not be operated efficiently.

We acknowledge the support of ANPCyT, Argentina; YerPhI, Armenia; ARC, Australia; BMWFW and FWF, Austria; ANAS, Azerbaijan; SSTC, Belarus; CNPq and FAPESP, Brazil; NSERC, NRC and CFI, Canada; CERN; CONICYT, Chile; CAS, MOST and NSFC, China; COLCIENCIAS, Colombia; MSMT CR, MPO CR and VSC CR, Czech Republic; DNRF and DNSRC, Denmark; IN2P3-CNRS, CEA-DSM/IRFU, France; GNSF, Georgia; BMBF, HGF, and MPG, Germany; GSRT, Greece; RGC, Hong Kong SAR, China; ISF, I-CORE and Benoziyo Center, Israel; INFN, Italy; MEXT and JSPS, Japan; CNRST, Morocco; FOM and NWO, Netherlands; RCN, Norway; MNiSW and NCN, Poland; FCT, Portugal; MNE/IFA, Romania; MES of Russia and NRC KI, Russian Federation; JINR; MESTD, Serbia; MSSR, Slovakia; ARRS and MIZŠ, Slovenia; DST/NRF, South Africa; MINECO, Spain; SRC and Wallenberg Foundation, Sweden; SERI, SNSF and Cantons of Bern and Geneva, Switzerland; MOST, Taiwan; TAEK, Turkey; STFC, United Kingdom; DOE and NSF, United States of America. In addition, individual groups and members have received support from BCKDF, the Canada Council, CANARIE, CRC, Compute Canada, FQRNT, and the Ontario Innovation Trust, Canada; EPLANET, ERC, FP7, Horizon 2020 and Marie Skłodowska-Curie Actions, European Union; Investissements d'Avenir Labex and Idex, ANR, Région Auvergne and Fondation Partager le Savoir, France; DFG and AvH Foundation, Germany; Herakleitos, Thales and Aristeia programmes co-financed by EU-ESF and the Greek NSRF; BSF, GIF and Minerva, Israel; BRF, Norway;

JHEP08(2016)147

Generalitat de Catalunya, Generalitat Valenciana, Spain; the Royal Society and Leverhulme Trust, United Kingdom.

The crucial computing support from all WLCG partners is acknowledged gratefully, in particular from CERN, the ATLAS Tier-1 facilities at TRIUMF (Canada), NDGF (Denmark, Norway, Sweden), CC-IN2P3 (France), KIT/GridKA (Germany), INFN-CNAF (Italy), NL-T1 (Netherlands), PIC (Spain), ASGC (Taiwan), RAL (U.K.) and BNL (U.S.A.), the Tier-2 facilities worldwide and large non-WLCG resource providers. Major contributors of computing resources are listed in ref. [35].

JHEP08(2016)147

References

[1] J. Charles et al., *Predictions of selected flavour observables within the standard model*, *Phys. Rev.* **D 84** (2011) 033005 [arXiv:1106.4041] [INSPIRE].

[2] A. Lenz and U. Nierste, *Numerical updates of lifetimes and mixing parameters of B mesons*, arXiv:1102.4274 [INSPIRE].

[3] A. Lenz and U. Nierste, *Theoretical update of B_s-$\bar{B}_s$ mixing*, *JHEP* **06** (2007) 072 [hep-ph/0612167] [INSPIRE].

[4] D0 collaboration, V.M. Abazov et al., *Measurement of the CP-violating phase $\phi_s^{J/\psi\phi}$ using the flavor-tagged decay $B_s^0 \to J/\psi\phi$ in 8 fb^{-1} of $p\bar{p}$ collisions*, *Phys. Rev.* **D 85** (2012) 032006 [arXiv:1109.3166] [INSPIRE].

[5] CDF collaboration, T. Aaltonen et al., *Measurement of the bottom-strange meson mixing phase in the full CDF data set*, *Phys. Rev. Lett.* **109** (2012) 171802 [arXiv:1208.2967] [INSPIRE].

[6] LHCb collaboration, *Measurement of CP-violation and the B_s^0 meson decay width difference with $B_s^0 \to J/\psi K^+K^-$ and $B_s^0 \to J/\psi\pi^+\pi^-$ decays*, *Phys. Rev.* **D 87** (2013) 112010 [arXiv:1304.2600] [INSPIRE].

[7] LHCb collaboration, *Precision measurement of CP violation in $B_s^0 \to J/\psi K^+K^-$ decays*, *Phys. Rev. Lett.* **114** (2015) 041801 [arXiv:1411.3104] [INSPIRE].

[8] ATLAS collaboration, *Flavor tagged time-dependent angular analysis of the $B_s \to J/\psi\phi$ decay and extraction of $\Delta\Gamma_s$ and the weak phase ϕ_s in ATLAS*, *Phys. Rev.* **D 90** (2014) 052007 [arXiv:1407.1796] [INSPIRE].

[9] CMS collaboration, *Measurement of the CP-violating weak phase ϕ_s and the decay width difference $\Delta\Gamma_s$ using the $B_s^0 \to J/\psi\phi(1020)$ decay channel in pp collisions at $\sqrt{s} = 8$ TeV*, *Phys. Lett.* **B 757** (2016) 97 [arXiv:1507.07527] [INSPIRE].

[10] S. Stone and L. Zhang, *S-waves and the measurement of CP-violating phases in B_s decays*, *Phys. Rev.* **D 79** (2009) 074024 [arXiv:0812.2832] [INSPIRE].

[11] ATLAS collaboration, *The ATLAS experiment at the CERN Large Hadron Collider*, 2008 *JINST* **3** S08003 [INSPIRE].

[12] T. Sjöstrand, S. Mrenna and P.Z. Skands, *PYTHIA* 6.4 *physics and manual*, *JHEP* **05** (2006) 026 [hep-ph/0603175] [INSPIRE].

[13] T. Sjöstrand, S. Mrenna and P.Z. Skands, *A brief introduction to PYTHIA* 8.1, *Comput. Phys. Commun.* **178** (2008) 852 [arXiv:0710.3820] [INSPIRE].

[14] ATLAS collaboration, *ATLAS tunes of PYTHIA* 6 *and PYTHIA* 8 *for MC*11, ATL-PHYS-PUB-2011-009, CERN, Geneva Switzerland (2011).

[15] ATLAS collaboration, *The ATLAS simulation infrastructure*, *Eur. Phys. J.* **C 70** (2010) 823 [arXiv:1005.4568] [INSPIRE].

[16] GEANT4 collaboration, S. Agostinelli et al., *GEANT4: a simulation toolkit*, *Nucl. Instrum. Meth.* **A 506** (2003) 250 [INSPIRE].

[17] ATLAS collaboration, *Measurement of the differential cross-sections of inclusive, prompt and non-prompt J/ψ production in proton-proton collisions at $\sqrt{s} = 7$ TeV*, *Nucl. Phys.* **B 850** (2011) 387 [arXiv:1104.3038] [INSPIRE].

[18] Particle Data Group collaboration, K.A. Olive et al., *Review of particle physics*, *Chin. Phys.* **C 38** (2014) 090001 [INSPIRE].

[19] ATLAS collaboration, *ATLAS B-physics studies at increased LHC luminosity, potential for CP-violation measurement in the $B_s^0 \to J/\psi\phi$ decay*, ATL-PHYS-PUB-2013-010, CERN, Geneva Switzerland (2013).

[20] R.D. Field and R.P. Feynman, *A parametrization of the properties of quark jets*, *Nucl. Phys.* **B 136** (1978) 1 [INSPIRE].

[21] ATLAS collaboration, *Jet charge studies with the ATLAS detector using $\sqrt{s} = 8$ TeV proton-proton collision data*, ATLAS-CONF-2013-086, CERN, Geneva Switzerland (2013).

[22] ATLAS collaboration, *Electron performance measurements with the ATLAS detector using the* 2010 *LHC proton-proton collision data*, *Eur. Phys. J.* **C 72** (2012) 1909 [arXiv:1110.3174] [INSPIRE].

[23] ATLAS collaboration, *Calibration of the performance of b-tagging for c and light-flavour jets in the* 2012 *ATLAS data*, ATLAS-CONF-2014-046, CERN, Geneva Switzerland (2014).

[24] M. Cacciari, G.P. Salam and G. Soyez, *The anti-k_t jet clustering algorithm*, *JHEP* **04** (2008) 063 [arXiv:0802.1189] [INSPIRE].

[25] ATLAS collaboration, *Time-dependent angular analysis of the decay $B_s^0 \to J/\psi\phi$ and extraction of $\Delta\Gamma_s$ and the CP-violating weak phase ϕ_s by ATLAS*, *JHEP* **12** (2012) 072 [arXiv:1208.0572] [INSPIRE].

[26] A.S. Dighe, I. Dunietz and R. Fleischer, *Extracting CKM phases and B_s^0-$\bar{B}_s^0$ mixing parameters from angular distributions of nonleptonic B decays*, *Eur. Phys. J.* **C 6** (1999) 647 [hep-ph/9804253] [INSPIRE].

[27] LHCb collaboration, *Updated average f_s/f_d b-hadron production fraction ratio for* 7 *TeV pp collisions*, LHCb-CONF-2013-011, CERN, Geneva Switzerland (2013).

[28] BaBar collaboration, B. Aubert et al., *Search for the $Z(4430)^-$ at BABAR*, *Phys. Rev.* **D 79** (2009) 112001 [arXiv:0811.0564] [INSPIRE].

[29] LHCb collaboration, *Study of the kinematic dependences of Λ_b^0 production in pp collisions and a measurement of the $\Lambda_b^0 \to \Lambda_c^+\pi^-$ branching fraction*, *JHEP* **08** (2014) 143 [arXiv:1405.6842] [INSPIRE].

JHEP08(2016)147

[30] LHCb collaboration, *Study of the production of Λ_b^0 and $\overline{B}^0$ hadrons in pp collisions and first measurement of the $\Lambda_b^0 \to J/\psi p K^-$ branching fraction*, *Chin. Phys.* **C 40** (2016) 011001 [arXiv:1509.00292] [INSPIRE].

[31] LHCb collaboration, *Observation of $J/\psi p$ resonances consistent with pentaquark states in $\Lambda_b^0 \to J/\psi K^- p$ decays*, *Phys. Rev. Lett.* **115** (2015) 072001 [arXiv:1507.03414] [INSPIRE].

[32] LHCb collaboration, *Measurement of the polarization amplitudes in $B^0 \to J/\psi K^*(892)^0$ decays*, *Phys. Rev.* **D 88** (2013) 052002 [arXiv:1307.2782] [INSPIRE].

[33] LHCb collaboration, *Determination of the sign of the decay width difference in the B_s system*, *Phys. Rev. Lett.* **108** (2012) 241801 [arXiv:1202.4717] [INSPIRE].

[34] R. Nisius, *On the combination of correlated estimates of a physics observable*, *Eur. Phys. J.* **C 74** (2014) 3004 [arXiv:1402.4016] [INSPIRE].

[35] ATLAS collaboration, *ATLAS computing acknowledgements* 2016–2017, ATL-GEN-PUB-2016-002, CERN, Geneva Switzerland (2016).

JHEP08(2016)147

The ATLAS collaboration

G. Aad[85], B. Abbott[113], J. Abdallah[151], O. Abdinov[11], R. Aben[107], M. Abolins[90], O.S. AbouZeid[158], H. Abramowicz[153], H. Abreu[152], R. Abreu[116], Y. Abulaiti[146a,146b], B.S. Acharya[164a,164b,a], L. Adamczyk[38a], D.L. Adams[25], J. Adelman[108], S. Adomeit[100], T. Adye[131], A.A. Affolder[74], T. Agatonovic-Jovin[13], J. Agricola[54], J.A. Aguilar-Saavedra[126a,126f], S.P. Ahlen[22], F. Ahmadov[65,b], G. Aielli[133a,133b], H. Akerstedt[146a,146b], T.P.A. Åkesson[81], A.V. Akimov[96], G.L. Alberghi[20a,20b], J. Albert[169], S. Albrand[55], M.J. Alconada Verzini[71], M. Aleksa[30], I.N. Aleksandrov[65], C. Alexa[26a], G. Alexander[153], T. Alexopoulos[10], M. Alhroob[113], G. Alimonti[91a], L. Alio[85], J. Alison[31], S.P. Alkire[35], B.M.M. Allbrooke[149], P.P. Allport[74], A. Aloisio[104a,104b], A. Alonso[36], F. Alonso[71], C. Alpigiani[76], A. Altheimer[35], B. Alvarez Gonzalez[30], D. Álvarez Piqueras[167], M.G. Alviggi[104a,104b], B.T. Amadio[15], K. Amako[66], Y. Amaral Coutinho[24a], C. Amelung[23], D. Amidei[89], S.P. Amor Dos Santos[126a,126c], A. Amorim[126a,126b], S. Amoroso[48], N. Amram[153], G. Amundsen[23], C. Anastopoulos[139], L.S. Ancu[49], N. Andari[108], T. Andeen[35], C.F. Anders[58b], G. Anders[30], J.K. Anders[74], K.J. Anderson[31], A. Andreazza[91a,91b], V. Andrei[58a], S. Angelidakis[9], I. Angelozzi[107], P. Anger[44], A. Angerami[35], F. Anghinolfi[30], A.V. Anisenkov[109,c], N. Anjos[12], A. Annovi[124a,124b], M. Antonelli[47], A. Antonov[98], J. Antos[144b], F. Anulli[132a], M. Aoki[66], L. Aperio Bella[18], G. Arabidze[90], Y. Arai[66], J.P. Araque[126a], A.T.H. Arce[45], F.A. Arduh[71], J-F. Arguin[95], S. Argyropoulos[42], M. Arik[19a], A.J. Armbruster[30], O. Arnaez[30], V. Arnal[82], H. Arnold[48], M. Arratia[28], O. Arslan[21], A. Artamonov[97], G. Artoni[23], S. Asai[155], N. Asbah[42], A. Ashkenazi[153], B. Åsman[146a,146b], L. Asquith[149], K. Assamagan[25], R. Astalos[144a], M. Atkinson[165], N.B. Atlay[141], K. Augsten[128], M. Aurousseau[145b], G. Avolio[30], B. Axen[15], M.K. Ayoub[117], G. Azuelos[95,d], M.A. Baak[30], A.E. Baas[58a], M.J. Baca[18], C. Bacci[134a,134b], H. Bachacou[136], K. Bachas[154], M. Backes[30], M. Backhaus[30], P. Bagiacchi[132a,132b], P. Bagnaia[132a,132b], Y. Bai[33a], T. Bain[35], J.T. Baines[131], O.K. Baker[176], E.M. Baldin[109,c], P. Balek[129], T. Balestri[148], F. Balli[84], E. Banas[39], Sw. Banerjee[173], A.A.E. Bannoura[175], H.S. Bansil[18], L. Barak[30], E.L. Barberio[88], D. Barberis[50a,50b], M. Barbero[85], T. Barillari[101], M. Barisonzi[164a,164b], T. Barklow[143], N. Barlow[28], S.L. Barnes[84], B.M. Barnett[131], R.M. Barnett[15], Z. Barnovska[5], A. Baroncelli[134a], G. Barone[23], A.J. Barr[120], F. Barreiro[82], J. Barreiro Guimarães da Costa[57], R. Bartoldus[143], A.E. Barton[72], P. Bartos[144a], A. Basalaev[123], A. Bassalat[117], A. Basye[165], R.L. Bates[53], S.J. Batista[158], J.R. Batley[28], M. Battaglia[137], M. Bauce[132a,132b], F. Bauer[136], H.S. Bawa[143,e], J.B. Beacham[111], M.D. Beattie[72], T. Beau[80], P.H. Beauchemin[161], R. Beccherle[124a,124b], P. Bechtle[21], H.P. Beck[17,f], K. Becker[120], M. Becker[83], S. Becker[100], M. Beckingham[170], C. Becot[117], A.J. Beddall[19b], A. Beddall[19b], V.A. Bednyakov[65], C.P. Bee[148], L.J. Beemster[107], T.A. Beermann[175], M. Begel[25], J.K. Behr[120], C. Belanger-Champagne[87], W.H. Bell[49], G. Bella[153], L. Bellagamba[20a], A. Bellerive[29], M. Bellomo[86], K. Belotskiy[98], O. Beltramello[30], O. Benary[153], D. Benchekroun[135a], M. Bender[100], K. Bendtz[146a,146b], N. Benekos[10], Y. Benhammou[153], E. Benhar Noccioli[49], J.A. Benitez Garcia[159b], D.P. Benjamin[45], J.R. Bensinger[23], S. Bentvelsen[107], L. Beresford[120], M. Beretta[47], D. Berge[107], E. Bergeaas Kuutmann[166], N. Berger[5], F. Berghaus[169], J. Beringer[15], C. Bernard[22], N.R. Bernard[86], C. Bernius[110], F.U. Bernlochner[21], T. Berry[77], P. Berta[129], C. Bertella[83], G. Bertoli[146a,146b], F. Bertolucci[124a,124b], C. Bertsche[113], D. Bertsche[113], M.I. Besana[91a], G.J. Besjes[36], O. Bessidskaia Bylund[146a,146b], M. Bessner[42], N. Besson[136], C. Betancourt[48], S. Bethke[101], A.J. Bevan[76], W. Bhimji[15], R.M. Bianchi[125], L. Bianchini[23], M. Bianco[30], O. Biebel[100], D. Biedermann[16], S.P. Bieniek[78], M. Biglietti[134a], J. Bilbao De Mendizabal[49], H. Bilokon[47], M. Bindi[54], S. Binet[117], A. Bingul[19b], C. Bini[132a,132b], S. Biondi[20a,20b], C.W. Black[150], J.E. Black[143], K.M. Black[22], D. Blackburn[138], R.E. Blair[6], J.-B. Blanchard[136],

JHEP08(2016)147

J.E. Blanco[77], T. Blazek[144a], I. Bloch[42], C. Blocker[23], W. Blum[83,*], U. Blumenschein[54], G.J. Bobbink[107], V.S. Bobrovnikov[109,c], S.S. Bocchetta[81], A. Bocci[45], C. Bock[100], M. Boehler[48], J.A. Bogaerts[30], D. Bogavac[13], A.G. Bogdanchikov[109], C. Bohm[146a], V. Boisvert[77], T. Bold[38a], V. Boldea[26a], A.S. Boldyrev[99], M. Bomben[80], M. Bona[76], M. Boonekamp[136], A. Borisov[130], G. Borissov[72], S. Borroni[42], J. Bortfeldt[100], V. Bortolotto[60a,60b,60c], K. Bos[107], D. Boscherini[20a], M. Bosman[12], J. Boudreau[125], J. Bouffard[2], E.V. Bouhova-Thacker[72], D. Boumediene[34], C. Bourdarios[117], N. Bousson[114], A. Boveia[30], J. Boyd[30], I.R. Boyko[65], I. Bozic[13], J. Bracinik[18], A. Brandt[8], G. Brandt[54], O. Brandt[58a], U. Bratzler[156], B. Brau[86], J.E. Brau[116], H.M. Braun[175,*], S.F. Brazzale[164a,164c], W.D. Breaden Madden[53], K. Brendlinger[122], A.J. Brennan[88], L. Brenner[107], R. Brenner[166], S. Bressler[172], K. Bristow[145c], T.M. Bristow[46], D. Britton[53], D. Britzger[42], F.M. Brochu[28], I. Brock[21], R. Brock[90], J. Bronner[101], G. Brooijmans[35], T. Brooks[77], W.K. Brooks[32b], J. Brosamer[15], E. Brost[116], J. Brown[55], P.A. Bruckman de Renstrom[39], D. Bruncko[144b], R. Bruneliere[48], A. Bruni[20a], G. Bruni[20a], M. Bruschi[20a], N. Bruscino[21], L. Bryngemark[81], T. Buanes[14], Q. Buat[142], P. Buchholz[141], A.G. Buckley[53], S.I. Buda[26a], I.A. Budagov[65], F. Buehrer[48], L. Bugge[119], M.K. Bugge[119], O. Bulekov[98], D. Bullock[8], H. Burckhart[30], S. Burdin[74], B. Burghgrave[108], S. Burke[131], I. Burmeister[43], E. Busato[34], D. Büscher[48], V. Büscher[83], P. Bussey[53], J.M. Butler[22], A.I. Butt[3], C.M. Buttar[53], J.M. Butterworth[78], P. Butti[107], W. Buttinger[25], A. Buzatu[53], A.R. Buzykaev[109,c], S. Cabrera Urbán[167], D. Caforio[128], V.M. Cairo[37a,37b], O. Cakir[4a], N. Calace[49], P. Calafiura[15], A. Calandri[136], G. Calderini[80], P. Calfayan[100], L.P. Caloba[24a], D. Calvet[34], S. Calvet[34], R. Camacho Toro[31], S. Camarda[42], P. Camarri[133a,133b], D. Cameron[119], R. Caminal Armadans[165], S. Campana[30], M. Campanelli[78], A. Campoverde[148], V. Canale[104a,104b], A. Canepa[159a], M. Cano Bret[33e], J. Cantero[82], R. Cantrill[126a], T. Cao[40], M.D.M. Capeans Garrido[30], I. Caprini[26a], M. Caprini[26a], M. Capua[37a,37b], R. Caputo[83], R. Cardarelli[133a], F. Cardillo[48], T. Carli[30], G. Carlino[104a], L. Carminati[91a,91b], S. Caron[106], E. Carquin[32a], G.D. Carrillo-Montoya[8], J.R. Carter[28], J. Carvalho[126a,126c], D. Casadei[78], M.P. Casado[12], M. Casolino[12], E. Castaneda-Miranda[145b], A. Castelli[107], V. Castillo Gimenez[167], N.F. Castro[126a,g], P. Catastini[57], A. Catinaccio[30], J.R. Catmore[119], A. Cattai[30], J. Caudron[83], V. Cavaliere[165], D. Cavalli[91a], M. Cavalli-Sforza[12], V. Cavasinni[124a,124b], F. Ceradini[134a,134b], B.C. Cerio[45], K. Cerny[129], A.S. Cerqueira[24b], A. Cerri[149], L. Cerrito[76], F. Cerutti[15], M. Cerv[30], A. Cervelli[17], S.A. Cetin[19c], A. Chafaq[135a], D. Chakraborty[108], I. Chalupkova[129], P. Chang[165], J.D. Chapman[28], D.G. Charlton[18], C.C. Chau[158], C.A. Chavez Barajas[149], S. Cheatham[152], A. Chegwidden[90], S. Chekanov[6], S.V. Chekulaev[159a], G.A. Chelkov[65,h], M.A. Chelstowska[89], C. Chen[64], H. Chen[25], K. Chen[148], L. Chen[33d,i], S. Chen[33c], X. Chen[33f], Y. Chen[67], H.C. Cheng[89], Y. Cheng[31], A. Cheplakov[65], E. Cheremushkina[130], R. Cherkaoui El Moursli[135e], V. Chernyatin[25,*], E. Cheu[7], L. Chevalier[136], V. Chiarella[47], G. Chiarelli[124a,124b], J.T. Childers[6], G. Chiodini[73a], A.S. Chisholm[18], R.T. Chislett[78], A. Chitan[26a], M.V. Chizhov[65], K. Choi[61], S. Chouridou[9], B.K.B. Chow[100], V. Christodoulou[78], D. Chromek-Burckhart[30], J. Chudoba[127], A.J. Chuinard[87], J.J. Chwastowski[39], L. Chytka[115], G. Ciapetti[132a,132b], A.K. Ciftci[4a], D. Cinca[53], V. Cindro[75], I.A. Cioara[21], A. Ciocio[15], Z.H. Citron[172], M. Ciubancan[26a], A. Clark[49], B.L. Clark[57], P.J. Clark[46], R.N. Clarke[15], W. Cleland[125], C. Clement[146a,146b], Y. Coadou[85], M. Cobal[164a,164c], A. Coccaro[49], J. Cochran[64], L. Coffey[23], J.G. Cogan[143], L. Colasurdo[106], B. Cole[35], S. Cole[108], A.P. Colijn[107], J. Collot[55], T. Colombo[58c], G. Compostella[101], P. Conde Muiño[126a,126b], E. Coniavitis[48], S.H. Connell[145b], I.A. Connelly[77], S.M. Consonni[91a,91b], V. Consorti[48], S. Constantinescu[26a], C. Conta[121a,121b], G. Conti[30], F. Conventi[104a,j], M. Cooke[15], B.D. Cooper[78], A.M. Cooper-Sarkar[120], T. Cornelissen[175], M. Corradi[20a], F. Corriveau[87,k], A. Corso-Radu[163], A. Cortes-Gonzalez[12], G. Cortiana[101], G. Costa[91a], M.J. Costa[167], D. Costanzo[139], D. Côté[8], G. Cottin[28], G. Cowan[77], B.E. Cox[84], K. Cranmer[110], G. Cree[29],

JHEP08(2016)147

S. Crépé-Renaudin[55], F. Crescioli[80], W.A. Cribbs[146a,146b], M. Crispin Ortuzar[120], M. Cristinziani[21], V. Croft[106], G. Crosetti[37a,37b], T. Cuhadar Donszelmann[139], J. Cummings[176], M. Curatolo[47], C. Cuthbert[150], H. Czirr[141], P. Czodrowski[3], S. D'Auria[53], M. D'Onofrio[74], M.J. Da Cunha Sargedas De Sousa[126a,126b], C. Da Via[84], W. Dabrowski[38a], A. Dafinca[120], T. Dai[89], O. Dale[14], F. Dallaire[95], C. Dallapiccola[86], M. Dam[36], J.R. Dandoy[31], N.P. Dang[48], A.C. Daniells[18], M. Danninger[168], M. Dano Hoffmann[136], V. Dao[48], G. Darbo[50a], S. Darmora[8], J. Dassoulas[3], A. Dattagupta[61], W. Davey[21], C. David[169], T. Davidek[129], E. Davies[120,l], M. Davies[153], P. Davison[78], Y. Davygora[58a], E. Dawe[88], I. Dawson[139], R.K. Daya-Ishmukhametova[86], K. De[8], R. de Asmundis[104a], A. De Benedetti[113], S. De Castro[20a,20b], S. De Cecco[80], N. De Groot[106], P. de Jong[107], H. De la Torre[82], F. De Lorenzi[64], L. De Nooij[107], D. De Pedis[132a], A. De Salvo[132a], U. De Sanctis[149], A. De Santo[149], J.B. De Vivie De Regie[117], W.J. Dearnaley[72], R. Debbe[25], C. Debenedetti[137], D.V. Dedovich[65], I. Deigaard[107], J. Del Peso[82], T. Del Prete[124a,124b], D. Delgove[117], F. Deliot[136], C.M. Delitzsch[49], M. Deliyergiyev[75], A. Dell'Acqua[30], L. Dell'Asta[22], M. Dell'Orso[124a,124b], M. Della Pietra[104a,j], D. della Volpe[49], M. Delmastro[5], P.A. Delsart[55], C. Deluca[107], D.A. DeMarco[158], S. Demers[176], M. Demichev[65], A. Demilly[80], S.P. Denisov[130], D. Derendarz[39], J.E. Derkaoui[135d], F. Derue[80], P. Dervan[74], K. Desch[21], C. Deterre[42], P.O. Deviveiros[30], A. Dewhurst[131], S. Dhaliwal[23], A. Di Ciaccio[133a,133b], L. Di Ciaccio[5], A. Di Domenico[132a,132b], C. Di Donato[104a,104b], A. Di Girolamo[30], B. Di Girolamo[30], A. Di Mattia[152], B. Di Micco[134a,134b], R. Di Nardo[47], A. Di Simone[48], R. Di Sipio[158], D. Di Valentino[29], C. Diaconu[85], M. Diamond[158], F.A. Dias[46], M.A. Diaz[32a], E.B. Diehl[89], J. Dietrich[16], S. Diglio[85], A. Dimitrievska[13], J. Dingfelder[21], P. Dita[26a], S. Dita[26a], F. Dittus[30], F. Djama[85], T. Djobava[51b], J.I. Djuvsland[58a], M.A.B. do Vale[24c], D. Dobos[30], M. Dobre[26a], C. Doglioni[81], T. Dohmae[155], J. Dolejsi[129], Z. Dolezal[129], B.A. Dolgoshein[98,*], M. Donadelli[24d], S. Donati[124a,124b], P. Dondero[121a,121b], J. Donini[34], J. Dopke[131], A. Doria[104a], M.T. Dova[71], A.T. Doyle[53], E. Drechsler[54], M. Dris[10], E. Dubreuil[34], E. Duchovni[172], G. Duckeck[100], O.A. Ducu[26a,85], D. Duda[107], A. Dudarev[30], L. Duflot[117], L. Duguid[77], M. Dührssen[30], M. Dunford[58a], H. Duran Yildiz[4a], M. Düren[52], A. Durglishvili[51b], D. Duschinger[44], M. Dyndal[38a], C. Eckardt[42], K.M. Ecker[101], R.C. Edgar[89], W. Edson[2], N.C. Edwards[46], W. Ehrenfeld[21], T. Eifert[30], G. Eigen[14], K. Einsweiler[15], T. Ekelof[166], M. El Kacimi[135c], M. Ellert[166], S. Elles[5], F. Ellinghaus[175], A.A. Elliot[169], N. Ellis[30], J. Elmsheuser[100], M. Elsing[30], D. Emeliyanov[131], Y. Enari[155], O.C. Endner[83], M. Endo[118], J. Erdmann[43], A. Ereditato[17], G. Ernis[175], J. Ernst[2], M. Ernst[25], S. Errede[165], E. Ertel[83], M. Escalier[117], H. Esch[43], C. Escobar[125], B. Esposito[47], A.I. Etienvre[136], E. Etzion[153], H. Evans[61], A. Ezhilov[123], L. Fabbri[20a,20b], G. Facini[31], R.M. Fakhrutdinov[130], S. Falciano[132a], R.J. Falla[78], J. Faltova[129], Y. Fang[33a], M. Fanti[91a,91b], A. Farbin[8], A. Farilla[134a], T. Farooque[12], S. Farrell[15], S.M. Farrington[170], P. Farthouat[30], F. Fassi[135e], P. Fassnacht[30], D. Fassouliotis[9], M. Faucci Giannelli[77], A. Favareto[50a,50b], L. Fayard[117], P. Federic[144a], O.L. Fedin[123,m], W. Fedorko[168], S. Feigl[30], L. Feligioni[85], C. Feng[33d], E.J. Feng[6], H. Feng[89], A.B. Fenyuk[130], L. Feremenga[8], P. Fernandez Martinez[167], S. Fernandez Perez[30], J. Ferrando[53], A. Ferrari[166], P. Ferrari[107], R. Ferrari[121a], D.E. Ferreira de Lima[53], A. Ferrer[167], D. Ferrere[49], C. Ferretti[89], A. Ferretto Parodi[50a,50b], M. Fiascaris[31], F. Fiedler[83], A. Filipčič[75], M. Filipuzzi[42], F. Filthaut[106], M. Fincke-Keeler[169], K.D. Finelli[150], M.C.N. Fiolhais[126a,126c], L. Fiorini[167], A. Firan[40], A. Fischer[2], C. Fischer[12], J. Fischer[175], W.C. Fisher[90], E.A. Fitzgerald[23], N. Flaschel[42], I. Fleck[141], P. Fleischmann[89], S. Fleischmann[175], G.T. Fletcher[139], G. Fletcher[76], R.R.M. Fletcher[122], T. Flick[175], A. Floderus[81], L.R. Flores Castillo[60a], M.J. Flowerdew[101], A. Formica[136], A. Forti[84], D. Fournier[117], H. Fox[72], S. Fracchia[12], P. Francavilla[80], M. Franchini[20a,20b], D. Francis[30], L. Franconi[119], M. Franklin[57], M. Frate[163], M. Fraternali[121a,121b], D. Freeborn[78], S.T. French[28], F. Friedrich[44], D. Froidevaux[30],

JHEP08(2016)147

J.A. Frost[120], C. Fukunaga[156], E. Fullana Torregrosa[83], B.G. Fulsom[143], T. Fusayasu[102], J. Fuster[167], C. Gabaldon[55], O. Gabizon[175], A. Gabrielli[20a,20b], A. Gabrielli[132a,132b], G.P. Gach[38a], S. Gadatsch[107], S. Gadomski[49], G. Gagliardi[50a,50b], P. Gagnon[61], C. Galea[106], B. Galhardo[126a,126c], E.J. Gallas[120], B.J. Gallop[131], P. Gallus[128], G. Galster[36], K.K. Gan[111], J. Gao[33b,85], Y. Gao[46], Y.S. Gao[143,e], F.M. Garay Walls[46], F. Garberson[176], C. García[167], J.E. García Navarro[167], M. Garcia-Sciveres[15], R.W. Gardner[31], N. Garelli[143], V. Garonne[119], C. Gatti[47], A. Gaudiello[50a,50b], G. Gaudio[121a], B. Gaur[141], L. Gauthier[95], P. Gauzzi[132a,132b], I.L. Gavrilenko[96], C. Gay[168], G. Gaycken[21], E.N. Gazis[10], P. Ge[33d], Z. Gecse[168], C.N.P. Gee[131], D.A.A. Geerts[107], Ch. Geich-Gimbel[21], M.P. Geisler[58a], C. Gemme[50a], M.H. Genest[55], S. Gentile[132a,132b], M. George[54], S. George[77], D. Gerbaudo[163], A. Gershon[153], S. Ghasemi[141], H. Ghazlane[135b], B. Giacobbe[20a], S. Giagu[132a,132b], V. Giangiobbe[12], P. Giannetti[124a,124b], B. Gibbard[25], S.M. Gibson[77], M. Gilchriese[15], T.P.S. Gillam[28], D. Gillberg[30], G. Gilles[34], D.M. Gingrich[3,d], N. Giokaris[9], M.P. Giordani[164a,164c], F.M. Giorgi[20a], F.M. Giorgi[16], P.F. Giraud[136], P. Giromini[47], D. Giugni[91a], C. Giuliani[48], M. Giulini[58b], B.K. Gjelsten[119], S. Gkaitatzis[154], I. Gkialas[154], E.L. Gkougkousis[117], L.K. Gladilin[99], C. Glasman[82], J. Glatzer[30], P.C.F. Glaysher[46], A. Glazov[42], M. Goblirsch-Kolb[101], J.R. Goddard[76], J. Godlewski[39], S. Goldfarb[89], T. Golling[49], D. Golubkov[130], A. Gomes[126a,126b,126d], R. Gonçalo[126a], J. Goncalves Pinto Firmino Da Costa[136], L. Gonella[21], S. González de la Hoz[167], G. Gonzalez Parra[12], S. Gonzalez-Sevilla[49], L. Goossens[30], P.A. Gorbounov[97], H.A. Gordon[25], I. Gorelov[105], B. Gorini[30], E. Gorini[73a,73b], A. Gorišek[75], E. Gornicki[39], A.T. Goshaw[45], C. Gössling[43], M.I. Gostkin[65], D. Goujdami[135c], A.G. Goussiou[138], N. Govender[145b], E. Gozani[152], H.M.X. Grabas[137], L. Graber[54], I. Grabowska-Bold[38a], P.O.J. Gradin[166], P. Grafström[20a,20b], K-J. Grahn[42], J. Gramling[49], E. Gramstad[119], S. Grancagnolo[16], V. Grassi[148], V. Gratchev[123], H.M. Gray[30], E. Graziani[134a], Z.D. Greenwood[79,n], K. Gregersen[78], I.M. Gregor[42], P. Grenier[143], J. Griffiths[8], A.A. Grillo[137], K. Grimm[72], S. Grinstein[12,o], Ph. Gris[34], J.-F. Grivaz[117], J.P. Grohs[44], A. Grohsjean[42], E. Gross[172], J. Grosse-Knetter[54], G.C. Grossi[79], Z.J. Grout[149], L. Guan[89], J. Guenther[128], F. Guescini[49], D. Guest[176], O. Gueta[153], E. Guido[50a,50b], T. Guillemin[117], S. Guindon[2], U. Gul[53], C. Gumpert[44], J. Guo[33e], Y. Guo[33b], S. Gupta[120], G. Gustavino[132a,132b], P. Gutierrez[113], N.G. Gutierrez Ortiz[78], C. Gutschow[44], C. Guyot[136], C. Gwenlan[120], C.B. Gwilliam[74], A. Haas[110], C. Haber[15], H.K. Hadavand[8], N. Haddad[135e], P. Haefner[21], S. Hageböck[21], Z. Hajduk[39], H. Hakobyan[177], M. Haleem[42], J. Haley[114], D. Hall[120], G. Halladjian[90], G.D. Hallewell[85], K. Hamacher[175], P. Hamal[115], K. Hamano[169], M. Hamer[54], A. Hamilton[145a], G.N. Hamity[145c], P.G. Hamnett[42], L. Han[33b], K. Hanagaki[66,p], K. Hanawa[155], M. Hance[15], P. Hanke[58a], R. Hanna[136], J.B. Hansen[36], J.D. Hansen[36], M.C. Hansen[21], P.H. Hansen[36], K. Hara[160], A.S. Hard[173], T. Harenberg[175], F. Hariri[117], S. Harkusha[92], R.D. Harrington[46], P.F. Harrison[170], F. Hartjes[107], M. Hasegawa[67], S. Hasegawa[103], Y. Hasegawa[140], A. Hasib[113], S. Hassani[136], S. Haug[17], R. Hauser[90], L. Hauswald[44], M. Havranek[127], C.M. Hawkes[18], R.J. Hawkings[30], A.D. Hawkins[81], T. Hayashi[160], D. Hayden[90], C.P. Hays[120], J.M. Hays[76], H.S. Hayward[74], S.J. Haywood[131], S.J. Head[18], T. Heck[83], V. Hedberg[81], L. Heelan[8], S. Heim[122], T. Heim[175], B. Heinemann[15], L. Heinrich[110], J. Hejbal[127], L. Helary[22], S. Hellman[146a,146b], D. Hellmich[21], C. Helsens[12], J. Henderson[120], R.C.W. Henderson[72], Y. Heng[173], C. Hengler[42], S. Henkelmann[168], A. Henrichs[176], A.M. Henriques Correia[30], S. Henrot-Versille[117], G.H. Herbert[16], Y. Hernández Jiménez[167], R. Herrberg-Schubert[16], G. Herten[48], R. Hertenberger[100], L. Hervas[30], G.G. Hesketh[78], N.P. Hessey[107], J.W. Hetherly[40], R. Hickling[76], E. Higón-Rodriguez[167], E. Hill[169], J.C. Hill[28], K.H. Hiller[42], S.J. Hillier[18], I. Hinchliffe[15], E. Hines[122], R.R. Hinman[15], M. Hirose[157], D. Hirschbuehl[175], J. Hobbs[148], N. Hod[107], M.C. Hodgkinson[139], P. Hodgson[139], A. Hoecker[30], M.R. Hoeferkamp[105], F. Hoenig[100], M. Hohlfeld[83], D. Hohn[21], T.R. Holmes[15],

JHEP08(2016)147

M. Homann[43], T.M. Hong[125], L. Hooft van Huysduynen[110], W.H. Hopkins[116], Y. Horii[103], A.J. Horton[142], J-Y. Hostachy[55], S. Hou[151], A. Hoummada[135a], J. Howard[120], J. Howarth[42], M. Hrabovsky[115], I. Hristova[16], J. Hrivnac[117], T. Hryn'ova[5], A. Hrynevich[93], C. Hsu[145c], P.J. Hsu[151,q], S.-C. Hsu[138], D. Hu[35], Q. Hu[33b], X. Hu[89], Y. Huang[42], Z. Hubacek[128], F. Hubaut[85], F. Huegging[21], T.B. Huffman[120], E.W. Hughes[35], G. Hughes[72], M. Huhtinen[30], T.A. Hülsing[83], N. Huseynov[65,b], J. Huston[90], J. Huth[57], G. Iacobucci[49], G. Iakovidis[25], I. Ibragimov[141], L. Iconomidou-Fayard[117], E. Ideal[176], Z. Idrissi[135e], P. Iengo[30], O. Igonkina[107], T. Iizawa[171], Y. Ikegami[66], K. Ikematsu[141], M. Ikeno[66], Y. Ilchenko[31,r], D. Iliadis[154], N. Ilic[143], T. Ince[101], G. Introzzi[121a,121b], P. Ioannou[9], M. Iodice[134a], K. Iordanidou[35], V. Ippolito[57], A. Irles Quiles[167], C. Isaksson[166], M. Ishino[68], M. Ishitsuka[157], R. Ishmukhametov[111], C. Issever[120], S. Istin[19a], J.M. Iturbe Ponce[84], R. Iuppa[133a,133b], J. Ivarsson[81], W. Iwanski[39], H. Iwasaki[66], J.M. Izen[41], V. Izzo[104a], S. Jabbar[3], B. Jackson[122], M. Jackson[74], P. Jackson[1], M.R. Jaekel[30], V. Jain[2], K. Jakobs[48], S. Jakobsen[30], T. Jakoubek[127], J. Jakubek[128], D.O. Jamin[114], D.K. Jana[79], E. Jansen[78], R. Jansky[62], J. Janssen[21], M. Janus[170], G. Jarlskog[81], N. Javadov[65,b], T. Javůrek[48], L. Jeanty[15], J. Jejelava[51a,s], G.-Y. Jeng[150], D. Jennens[88], P. Jenni[48,t], J. Jentzsch[43], C. Jeske[170], S. Jézéquel[5], H. Ji[173], J. Jia[148], Y. Jiang[33b], S. Jiggins[78], J. Jimenez Pena[167], S. Jin[33a], A. Jinaru[26a], O. Jinnouchi[157], M.D. Joergensen[36], P. Johansson[139], K.A. Johns[7], K. Jon-And[146a,146b], G. Jones[170], R.W.L. Jones[72], T.J. Jones[74], J. Jongmanns[58a], P.M. Jorge[126a,126b], K.D. Joshi[84], J. Jovicevic[159a], X. Ju[173], C.A. Jung[43], P. Jussel[62], A. Juste Rozas[12,o], M. Kaci[167], A. Kaczmarska[39], M. Kado[117], H. Kagan[111], M. Kagan[143], S.J. Kahn[85], E. Kajomovitz[45], C.W. Kalderon[120], S. Kama[40], A. Kamenshchikov[130], N. Kanaya[155], S. Kaneti[28], V.A. Kantserov[98], J. Kanzaki[66], B. Kaplan[110], L.S. Kaplan[173], A. Kapliy[31], D. Kar[53], K. Karakostas[10], A. Karamaoun[3], N. Karastathis[10,107], M.J. Kareem[54], E. Karentzos[10], M. Karnevskiy[83], S.N. Karpov[65], Z.M. Karpova[65], K. Karthik[110], V. Kartvelishvili[72], A.N. Karyukhin[130], L. Kashif[173], R.D. Kass[111], A. Kastanas[14], Y. Kataoka[155], C. Kato[155], A. Katre[49], J. Katzy[42], K. Kawagoe[70], T. Kawamoto[155], G. Kawamura[54], S. Kazama[155], V.F. Kazanin[109,c], R. Keeler[169], R. Kehoe[40], J.S. Keller[42], J.J. Kempster[77], H. Keoshkerian[84], O. Kepka[127], B.P. Kerševan[75], S. Kersten[175], R.A. Keyes[87], F. Khalil-zada[11], H. Khandanyan[146a,146b], A. Khanov[114], A.G. Kharlamov[109,c], T.J. Khoo[28], V. Khovanskiy[97], E. Khramov[65], J. Khubua[51b,u], H.Y. Kim[8], H. Kim[146a,146b], S.H. Kim[160], Y.K. Kim[31], N. Kimura[154], O.M. Kind[16], B.T. King[74], M. King[167], S.B. King[168], J. Kirk[131], A.E. Kiryunin[101], T. Kishimoto[67], D. Kisielewska[38a], F. Kiss[48], K. Kiuchi[160], O. Kivernyk[136], E. Kladiva[144b], M.H. Klein[35], M. Klein[74], U. Klein[74], K. Kleinknecht[83], P. Klimek[146a,146b], A. Klimentov[25], R. Klingenberg[43], J.A. Klinger[139], T. Klioutchnikova[30], E.-E. Kluge[58a], P. Kluit[107], S. Kluth[101], J. Knapik[39], E. Kneringer[62], E.B.F.G. Knoops[85], A. Knue[53], A. Kobayashi[155], D. Kobayashi[157], T. Kobayashi[155], M. Kobel[44], M. Kocian[143], P. Kodys[129], T. Koffas[29], E. Koffeman[107], L.A. Kogan[120], S. Kohlmann[175], Z. Kohout[128], T. Kohriki[66], T. Koi[143], H. Kolanoski[16], I. Koletsou[5], A.A. Komar[96,*], Y. Komori[155], T. Kondo[66], N. Kondrashova[42], K. Köneke[48], A.C. König[106], T. Kono[66], R. Konoplich[110,v], N. Konstantinidis[78], R. Kopeliansky[152], S. Koperny[38a], L. Köpke[83], A.K. Kopp[48], K. Korcyl[39], K. Kordas[154], A. Korn[78], A.A. Korol[109,c], I. Korolkov[12], E.V. Korolkova[139], O. Kortner[101], S. Kortner[101], T. Kosek[129], V.V. Kostyukhin[21], V.M. Kotov[65], A. Kotwal[45], A. Kourkoumeli-Charalampidi[154], C. Kourkoumelis[9], V. Kouskoura[25], A. Koutsman[159a], R. Kowalewski[169], T.Z. Kowalski[38a], W. Kozanecki[136], A.S. Kozhin[130], V.A. Kramarenko[99], G. Kramberger[75], D. Krasnopevtsev[98], M.W. Krasny[80], A. Krasznahorkay[30], J.K. Kraus[21], A. Kravchenko[25], S. Kreiss[110], M. Kretz[58c], J. Kretzschmar[74], K. Kreutzfeldt[52], P. Krieger[158], K. Krizka[31], K. Kroeninger[43], H. Kroha[101], J. Kroll[122], J. Kroseberg[21], J. Krstic[13], U. Kruchonak[65], H. Krüger[21], N. Krumnack[64], A. Kruse[173], M.C. Kruse[45], M. Kruskal[22], T. Kubota[88], H. Kucuk[78], S. Kuday[4b], S. Kuehn[48], A. Kugel[58c],

JHEP08(2016)147

F. Kuger[174], A. Kuhl[137], T. Kuhl[42], V. Kukhtin[65], Y. Kulchitsky[92], S. Kuleshov[32b], M. Kuna[132a,132b], T. Kunigo[68], A. Kupco[127], H. Kurashige[67], Y.A. Kurochkin[92], V. Kus[127], E.S. Kuwertz[169], M. Kuze[157], J. Kvita[115], T. Kwan[169], D. Kyriazopoulos[139], A. La Rosa[137], J.L. La Rosa Navarro[24d], L. La Rotonda[37a,37b], C. Lacasta[167], F. Lacava[132a,132b], J. Lacey[29], H. Lacker[16], D. Lacour[80], V.R. Lacuesta[167], E. Ladygin[65], R. Lafaye[5], B. Laforge[80], T. Lagouri[176], S. Lai[54], L. Lambourne[78], S. Lammers[61], C.L. Lampen[7], W. Lampl[7], E. Lançon[136], U. Landgraf[48], M.P.J. Landon[76], V.S. Lang[58a], J.C. Lange[12], A.J. Lankford[163], F. Lanni[25], K. Lantzsch[21], A. Lanza[121a], S. Laplace[80], C. Lapoire[30], J.F. Laporte[136], T. Lari[91a], F. Lasagni Manghi[20a,20b], M. Lassnig[30], P. Laurelli[47], W. Lavrijsen[15], A.T. Law[137], P. Laycock[74], T. Lazovich[57], O. Le Dortz[80], E. Le Guirriec[85], E. Le Menedeu[12], M. LeBlanc[169], T. LeCompte[6], F. Ledroit-Guillon[55], C.A. Lee[145b], S.C. Lee[151], L. Lee[1], G. Lefebvre[80], M. Lefebvre[169], F. Legger[100], C. Leggett[15], A. Lehan[74], G. Lehmann Miotto[30], X. Lei[7], W.A. Leight[29], A. Leisos[154,w], A.G. Leister[176], M.A.L. Leite[24d], R. Leitner[129], D. Lellouch[172], B. Lemmer[54], K.J.C. Leney[78], T. Lenz[21], B. Lenzi[30], R. Leone[7], S. Leone[124a,124b], C. Leonidopoulos[46], S. Leontsinis[10], C. Leroy[95], C.G. Lester[28], M. Levchenko[123], J. Levêque[5], D. Levin[89], L.J. Levinson[172], M. Levy[18], A. Lewis[120], A.M. Leyko[21], M. Leyton[41], B. Li[33b,x], H. Li[148], H.L. Li[31], L. Li[45], L. Li[33e], S. Li[45], Y. Li[33c,y], Z. Liang[137], H. Liao[34], B. Liberti[133a], A. Liblong[158], P. Lichard[30], K. Lie[165], J. Liebal[21], W. Liebig[14], C. Limbach[21], A. Limosani[150], S.C. Lin[151,z], T.H. Lin[83], F. Linde[107], B.E. Lindquist[148], J.T. Linnemann[90], E. Lipeles[122], A. Lipniacka[14], M. Lisovyi[58b], T.M. Liss[165], D. Lissauer[25], A. Lister[168], A.M. Litke[137], B. Liu[151,aa], D. Liu[151], H. Liu[89], J. Liu[85], J.B. Liu[33b], K. Liu[85], L. Liu[165], M. Liu[45], M. Liu[33b], Y. Liu[33b], M. Livan[121a,121b], A. Lleres[55], J. Llorente Merino[82], S.L. Lloyd[76], F. Lo Sterzo[151], E. Lobodzinska[42], P. Loch[7], W.S. Lockman[137], F.K. Loebinger[84], A.E. Loevschall-Jensen[36], A. Loginov[176], T. Lohse[16], K. Lohwasser[42], M. Lokajicek[127], B.A. Long[22], J.D. Long[89], R.E. Long[72], K.A. Looper[111], L. Lopes[126a], D. Lopez Mateos[57], B. Lopez Paredes[139], I. Lopez Paz[12], J. Lorenz[100], N. Lorenzo Martinez[61], M. Losada[162], P. Loscutoff[15], P.J. Lösel[100], X. Lou[33a], A. Lounis[117], J. Love[6], P.A. Love[72], N. Lu[89], H.J. Lubatti[138], C. Luci[132a,132b], A. Lucotte[55], F. Luehring[61], W. Lukas[62], L. Luminari[132a], O. Lundberg[146a,146b], B. Lund-Jensen[147], D. Lynn[25], R. Lysak[127], E. Lytken[81], H. Ma[25], L.L. Ma[33d], G. Maccarrone[47], A. Macchiolo[101], C.M. Macdonald[139], J. Machado Miguens[122,126b], D. Macina[30], D. Madaffari[85], R. Madar[34], H.J. Maddocks[72], W.F. Mader[44], A. Madsen[166], S. Maeland[14], T. Maeno[25], A. Maevskiy[99], E. Magradze[54], K. Mahboubi[48], J. Mahlstedt[107], C. Maiani[136], C. Maidantchik[24a], A.A. Maier[101], T. Maier[100], A. Maio[126a,126b,126d], S. Majewski[116], Y. Makida[66], N. Makovec[117], B. Malaescu[80], Pa. Malecki[39], V.P. Maleev[123], F. Malek[55], U. Mallik[63], D. Malon[6], C. Malone[143], S. Maltezos[10], V.M. Malyshev[109], S. Malyukov[30], J. Mamuzic[42], G. Mancini[47], B. Mandelli[30], L. Mandelli[91a], I. Mandić[75], R. Mandrysch[63], J. Maneira[126a,126b], A. Manfredini[101], L. Manhaes de Andrade Filho[24b], J. Manjarres Ramos[159b], A. Mann[100], P.M. Manning[137], A. Manousakis-Katsikakis[9], B. Mansoulie[136], R. Mantifel[87], M. Mantoani[54], L. Mapelli[30], L. March[145c], G. Marchiori[80], M. Marcisovsky[127], C.P. Marino[169], M. Marjanovic[13], D.E. Marley[89], F. Marroquim[24a], S.P. Marsden[84], Z. Marshall[15], L.F. Marti[17], S. Marti-Garcia[167], B. Martin[90], T.A. Martin[170], V.J. Martin[46], B. Martin dit Latour[14], M. Martinez[12,o], S. Martin-Haugh[131], V.S. Martoiu[26a], A.C. Martyniuk[78], M. Marx[138], F. Marzano[132a], A. Marzin[30], L. Masetti[83], T. Mashimo[155], R. Mashinistov[96], J. Masik[84], A.L. Maslennikov[109,c], I. Massa[20a,20b], L. Massa[20a,20b], N. Massol[5], P. Mastrandrea[148], A. Mastroberardino[37a,37b], T. Masubuchi[155], P. Mättig[175], J. Mattmann[83], J. Maurer[26a], S.J. Maxfield[74], D.A. Maximov[109,c], R. Mazini[151], S.M. Mazza[91a,91b], L. Mazzaferro[133a,133b], G. Mc Goldrick[158], S.P. Mc Kee[89], A. McCarn[89], R.L. McCarthy[148], T.G. McCarthy[29], N.A. McCubbin[131], K.W. McFarlane[56,*], J.A. Mcfayden[78], G. Mchedlidze[54], S.J. McMahon[131], R.A. McPherson[169,k], M. Medinnis[42],

JHEP08(2016)147

S. Meehan[145a], S. Mehlhase[100], A. Mehta[74], K. Meier[58a], C. Meineck[100], B. Meirose[41], B.R. Mellado Garcia[145c], F. Meloni[17], A. Mengarelli[20a,20b], S. Menke[101], E. Meoni[161], K.M. Mercurio[57], S. Mergelmeyer[21], P. Mermod[49], L. Merola[104a,104b], C. Meroni[91a], F.S. Merritt[31], A. Messina[132a,132b], J. Metcalfe[25], A.S. Mete[163], C. Meyer[83], C. Meyer[122], J-P. Meyer[136], J. Meyer[107], R.P. Middleton[131], S. Miglioranzi[164a,164c], L. Mijović[21], G. Mikenberg[172], M. Mikestikova[127], M. Mikuž[75], M. Milesi[88], A. Milic[30], D.W. Miller[31], C. Mills[46], A. Milov[172], D.A. Milstead[146a,146b], A.A. Minaenko[130], Y. Minami[155], I.A. Minashvili[65], A.I. Mincer[110], B. Mindur[38a], M. Mineev[65], Y. Ming[173], L.M. Mir[12], T. Mitani[171], J. Mitrevski[100], V.A. Mitsou[167], A. Miucci[49], P.S. Miyagawa[139], J.U. Mjörnmark[81], T. Moa[146a,146b], K. Mochizuki[85], S. Mohapatra[35], W. Mohr[48], S. Molander[146a,146b], R. Moles-Valls[21], K. Mönig[42], C. Monini[55], J. Monk[36], E. Monnier[85], J. Montejo Berlingen[12], F. Monticelli[71], S. Monzani[132a,132b], R.W. Moore[3], N. Morange[117], D. Moreno[162], M. Moreno Llácer[54], P. Morettini[50a], M. Morgenstern[44], D. Mori[142], M. Morii[57], M. Morinaga[155], V. Morisbak[119], S. Moritz[83], A.K. Morley[150], G. Mornacchi[30], J.D. Morris[76], S.S. Mortensen[36], A. Morton[53], L. Morvaj[103], M. Mosidze[51b], J. Moss[111], K. Motohashi[157], R. Mount[143], E. Mountricha[25], S.V. Mouraviev[96,*], E.J.W. Moyse[86], S. Muanza[85], R.D. Mudd[18], F. Mueller[101], J. Mueller[125], R.S.P. Mueller[100], T. Mueller[28], D. Muenstermann[49], P. Mullen[53], G.A. Mullier[17], J.A. Murillo Quijada[18], W.J. Murray[170,131], H. Musheghyan[54], E. Musto[152], A.G. Myagkov[130,ab], M. Myska[128], B.P. Nachman[143], O. Nackenhorst[54], J. Nadal[54], K. Nagai[120], R. Nagai[157], Y. Nagai[85], K. Nagano[66], A. Nagarkar[111], Y. Nagasaka[59], K. Nagata[160], M. Nagel[101], E. Nagy[85], A.M. Nairz[30], Y. Nakahama[30], K. Nakamura[66], T. Nakamura[155], I. Nakano[112], H. Namasivayam[41], R.F. Naranjo Garcia[42], R. Narayan[31], T. Naumann[42], G. Navarro[162], R. Nayyar[7], H.A. Neal[89], P.Yu. Nechaeva[96], T.J. Neep[84], P.D. Nef[143], A. Negri[121a,121b], M. Negrini[20a], S. Nektarijevic[106], C. Nellist[117], A. Nelson[163], S. Nemecek[127], P. Nemethy[110], A.A. Nepomuceno[24a], M. Nessi[30,ac], M.S. Neubauer[165], M. Neumann[175], R.M. Neves[110], P. Nevski[25], P.R. Newman[18], D.H. Nguyen[6], R.B. Nickerson[120], R. Nicolaidou[136], B. Nicquevert[30], J. Nielsen[137], N. Nikiforou[35], A. Nikiforov[16], V. Nikolaenko[130,ab], I. Nikolic-Audit[80], K. Nikolopoulos[18], J.K. Nilsen[119], P. Nilsson[25], Y. Ninomiya[155], A. Nisati[132a], R. Nisius[101], T. Nobe[155], M. Nomachi[118], I. Nomidis[29], T. Nooney[76], S. Norberg[113], M. Nordberg[30], O. Novgorodova[44], S. Nowak[101], M. Nozaki[66], L. Nozka[115], K. Ntekas[10], G. Nunes Hanninger[88], T. Nunnemann[100], E. Nurse[78], F. Nuti[88], B.J. O'Brien[46], F. O'grady[7], D.C. O'Neil[142], V. O'Shea[53], F.G. Oakham[29,d], H. Oberlack[101], T. Obermann[21], J. Ocariz[80], A. Ochi[67], I. Ochoa[78], J.P. Ochoa-Ricoux[32a], S. Oda[70], S. Odaka[66], H. Ogren[61], A. Oh[84], S.H. Oh[45], C.C. Ohm[15], H. Ohman[166], H. Oide[30], W. Okamura[118], H. Okawa[160], Y. Okumura[31], T. Okuyama[66], A. Olariu[26a], S.A. Olivares Pino[46], D. Oliveira Damazio[25], E. Oliver Garcia[167], A. Olszewski[39], J. Olszowska[39], A. Onofre[126a,126e], P.U.E. Onyisi[31,r], C.J. Oram[159a], M.J. Oreglia[31], Y. Oren[153], D. Orestano[134a,134b], N. Orlando[154], C. Oropeza Barrera[53], R.S. Orr[158], B. Osculati[50a,50b], R. Ospanov[84], G. Otero y Garzon[27], H. Otono[70], M. Ouchrif[135d], E.A. Ouellette[169], F. Ould-Saada[119], A. Ouraou[136], K.P. Oussoren[107], Q. Ouyang[33a], A. Ovcharova[15], M. Owen[53], R.E. Owen[18], V.E. Ozcan[19a], N. Ozturk[8], K. Pachal[142], A. Pacheco Pages[12], C. Padilla Aranda[12], M. Pagáčová[48], S. Pagan Griso[15], E. Paganis[139], F. Paige[25], P. Pais[86], K. Pajchel[119], G. Palacino[159b], S. Palestini[30], M. Palka[38b], D. Pallin[34], A. Palma[126a,126b], Y.B. Pan[173], E. Panagiotopoulou[10], C.E. Pandini[80], J.G. Panduro Vazquez[77], P. Pani[146a,146b], S. Panitkin[25], D. Pantea[26a], L. Paolozzi[49], Th.D. Papadopoulou[10], K. Papageorgiou[154], A. Paramonov[6], D. Paredes Hernandez[154], M.A. Parker[28], K.A. Parker[139], F. Parodi[50a,50b], J.A. Parsons[35], U. Parzefall[48], E. Pasqualucci[132a], S. Passaggio[50a], F. Pastore[134a,134b,*], Fr. Pastore[77], G. Pásztor[29], S. Pataraia[175], N.D. Patel[150], J.R. Pater[84], T. Pauly[30], J. Pearce[169], B. Pearson[113], L.E. Pedersen[36], M. Pedersen[119], S. Pedraza Lopez[167],

JHEP08(2016)147

R. Pedro[126a,126b], S.V. Peleganchuk[109,c], D. Pelikan[166], O. Penc[127], C. Peng[33a], H. Peng[33b], B. Penning[31], J. Penwell[61], D.V. Perepelitsa[25], E. Perez Codina[159a], M.T. Pérez García-Estañ[167], L. Perini[91a,91b], H. Pernegger[30], S. Perrella[104a,104b], R. Peschke[42], V.D. Peshekhonov[65], K. Peters[30], R.F.Y. Peters[84], B.A. Petersen[30], T.C. Petersen[36], E. Petit[42], A. Petridis[146a,146b], C. Petridou[154], P. Petroff[117], E. Petrolo[132a], F. Petrucci[134a,134b], N.E. Pettersson[157], R. Pezoa[32b], P.W. Phillips[131], G. Piacquadio[143], E. Pianori[170], A. Picazio[49], E. Piccaro[76], M. Piccinini[20a,20b], M.A. Pickering[120], R. Piegaia[27], D.T. Pignotti[111], J.E. Pilcher[31], A.D. Pilkington[84], J. Pina[126a,126b,126d], M. Pinamonti[164a,164c,ad], J.L. Pinfold[3], A. Pingel[36], B. Pinto[126a], S. Pires[80], H. Pirumov[42], M. Pitt[172], C. Pizio[91a,91b], L. Plazak[144a], M.-A. Pleier[25], V. Pleskot[129], E. Plotnikova[65], P. Plucinski[146a,146b], D. Pluth[64], R. Poettgen[146a,146b], L. Poggioli[117], D. Pohl[21], G. Polesello[121a], A. Poley[42], A. Policicchio[37a,37b], R. Polifka[158], A. Polini[20a], C.S. Pollard[53], V. Polychronakos[25], K. Pommès[30], L. Pontecorvo[132a], B.G. Pope[90], G.A. Popeneciu[26b], D.S. Popovic[13], A. Poppleton[30], S. Pospisil[128], K. Potamianos[15], I.N. Potrap[65], C.J. Potter[149], C.T. Potter[116], G. Poulard[30], J. Poveda[30], V. Pozdnyakov[65], P. Pralavorio[85], A. Pranko[15], S. Prasad[30], S. Prell[64], D. Price[84], L.E. Price[6], M. Primavera[73a], S. Prince[87], M. Proissl[46], K. Prokofiev[60c], F. Prokoshin[32b], E. Protopapadaki[136], S. Protopopescu[25], J. Proudfoot[6], M. Przybycien[38a], E. Ptacek[116], D. Puddu[134a,134b], E. Pueschel[86], D. Puldon[148], M. Purohit[25,ae], P. Puzo[117], J. Qian[89], G. Qin[53], Y. Qin[84], A. Quadt[54], D.R. Quarrie[15], W.B. Quayle[164a,164b], M. Queitsch-Maitland[84], D. Quilty[53], S. Raddum[119], V. Radeka[25], V. Radescu[42], S.K. Radhakrishnan[148], P. Radloff[116], P. Rados[88], F. Ragusa[91a,91b], G. Rahal[178], S. Rajagopalan[25], M. Rammensee[30], C. Rangel-Smith[166], F. Rauscher[100], S. Rave[83], T. Ravenscroft[53], M. Raymond[30], A.L. Read[119], N.P. Readioff[74], D.M. Rebuzzi[121a,121b], A. Redelbach[174], G. Redlinger[25], R. Reece[137], K. Reeves[41], L. Rehnisch[16], J. Reichert[122], H. Reisin[27], M. Relich[163], C. Rembser[30], H. Ren[33a], A. Renaud[117], M. Rescigno[132a], S. Resconi[91a], O.L. Rezanova[109,c], P. Reznicek[129], R. Rezvani[95], R. Richter[101], S. Richter[78], E. Richter-Was[38b], O. Ricken[21], M. Ridel[80], P. Rieck[16], C.J. Riegel[175], J. Rieger[54], M. Rijssenbeek[148], A. Rimoldi[121a,121b], L. Rinaldi[20a], B. Ristić[49], E. Ritsch[30], I. Riu[12], F. Rizatdinova[114], E. Rizvi[76], S.H. Robertson[87,k], A. Robichaud-Veronneau[87], D. Robinson[28], J.E.M. Robinson[42], A. Robson[53], C. Roda[124a,124b], S. Roe[30], O. Røhne[119], S. Rolli[161], A. Romaniouk[98], M. Romano[20a,20b], S.M. Romano Saez[34], E. Romero Adam[167], N. Rompotis[138], M. Ronzani[48], L. Roos[80], E. Ros[167], S. Rosati[132a], K. Rosbach[48], P. Rose[137], P.L. Rosendahl[14], O. Rosenthal[141], V. Rossetti[146a,146b], E. Rossi[104a,104b], L.P. Rossi[50a], R. Rosten[138], M. Rotaru[26a], I. Roth[172], J. Rothberg[138], D. Rousseau[117], C.R. Royon[136], A. Rozanov[85], Y. Rozen[152], X. Ruan[145c], F. Rubbo[143], I. Rubinskiy[42], V.I. Rud[99], C. Rudolph[44], M.S. Rudolph[158], F. Rühr[48], A. Ruiz-Martinez[30], Z. Rurikova[48], N.A. Rusakovich[65], A. Ruschke[100], H.L. Russell[138], J.P. Rutherfoord[7], N. Ruthmann[48], Y.F. Ryabov[123], M. Rybar[165], G. Rybkin[117], N.C. Ryder[120], A.F. Saavedra[150], G. Sabato[107], S. Sacerdoti[27], A. Saddique[3], H.F-W. Sadrozinski[137], R. Sadykov[65], F. Safai Tehrani[132a], M. Sahinsoy[19a], M. Saimpert[136], T. Saito[155], H. Sakamoto[155], Y. Sakurai[171], G. Salamanna[134a,134b], A. Salamon[133a], M. Saleem[113], D. Salek[107], P.H. Sales De Bruin[138], D. Salihagic[101], A. Salnikov[143], J. Salt[167], D. Salvatore[37a,37b], F. Salvatore[149], A. Salvucci[106], A. Salzburger[30], D. Sammel[48], D. Sampsonidis[154], A. Sanchez[104a,104b], J. Sánchez[167], V. Sanchez Martinez[167], H. Sandaker[119], R.L. Sandbach[76], H.G. Sander[83], M.P. Sanders[100], M. Sandhoff[175], C. Sandoval[162], R. Sandstroem[101], D.P.C. Sankey[131], M. Sannino[50a,50b], A. Sansoni[47], C. Santoni[34], R. Santonico[133a,133b], H. Santos[126a], I. Santoyo Castillo[149], K. Sapp[125], A. Sapronov[65], J.G. Saraiva[126a,126d], B. Sarrazin[21], O. Sasaki[66], Y. Sasaki[155], K. Sato[160], G. Sauvage[5,*], E. Sauvan[5], G. Savage[77], P. Savard[158,d], C. Sawyer[131], L. Sawyer[79,n], J. Saxon[31], C. Sbarra[20a], A. Sbrizzi[20a,20b], T. Scanlon[78], D.A. Scannicchio[163], M. Scarcella[150], V. Scarfone[37a,37b], J. Schaarschmidt[172], P. Schacht[101], D. Schaefer[30], R. Schaefer[42], J. Schaeffer[83],

JHEP08(2016)147

S. Schaepe[21], S. Schaetzel[58b], U. Schäfer[83], A.C. Schaffer[117], D. Schaile[100], R.D. Schamberger[148], V. Scharf[58a], V.A. Schegelsky[123], D. Scheirich[129], M. Schernau[163], C. Schiavi[50a,50b], C. Schillo[48], M. Schioppa[37a,37b], S. Schlenker[30], E. Schmidt[48], K. Schmieden[30], C. Schmitt[83], S. Schmitt[58b], S. Schmitt[42], B. Schneider[159a], Y.J. Schnellbach[74], U. Schnoor[44], L. Schoeffel[136], A. Schoening[58b], B.D. Schoenrock[90], E. Schopf[21], A.L.S. Schorlemmer[54], M. Schott[83], D. Schouten[159a], J. Schovancova[8], S. Schramm[49], M. Schreyer[174], C. Schroeder[83], N. Schuh[83], M.J. Schultens[21], H.-C. Schultz-Coulon[58a], H. Schulz[16], M. Schumacher[48], B.A. Schumm[137], Ph. Schune[136], C. Schwanenberger[84], A. Schwartzman[143], T.A. Schwarz[89], Ph. Schwegler[101], H. Schweiger[84], Ph. Schwemling[136], R. Schwienhorst[90], J. Schwindling[136], T. Schwindt[21], F.G. Sciacca[17], E. Scifo[117], G. Sciolla[23], F. Scuri[124a,124b], F. Scutti[21], J. Searcy[89], G. Sedov[42], E. Sedykh[123], P. Seema[21], S.C. Seidel[105], A. Seiden[137], F. Seifert[128], J.M. Seixas[24a], G. Sekhniaidze[104a], K. Sekhon[89], S.J. Sekula[40], D.M. Seliverstov[123,*], N. Semprini-Cesari[20a,20b], C. Serfon[30], L. Serin[117], L. Serkin[164a,164b], T. Serre[85], M. Sessa[134a,134b], R. Seuster[159a], H. Severini[113], T. Sfiligoj[75], F. Sforza[30], A. Sfyrla[30], E. Shabalina[54], M. Shamim[116], L.Y. Shan[33a], R. Shang[165], J.T. Shank[22], M. Shapiro[15], P.B. Shatalov[97], K. Shaw[164a,164b], S.M. Shaw[84], A. Shcherbakova[146a,146b], C.Y. Shehu[149], P. Sherwood[78], L. Shi[151,af], S. Shimizu[67], C.O. Shimmin[163], M. Shimojima[102], M. Shiyakova[65], A. Shmeleva[96], D. Shoaleh Saadi[95], M.J. Shochet[31], S. Shojaii[91a,91b], S. Shrestha[111], E. Shulga[98], M.A. Shupe[7], S. Shushkevich[42], P. Sicho[127], P.E. Sidebo[147], O. Sidiropoulou[174], D. Sidorov[114], A. Sidoti[20a,20b], F. Siegert[44], Dj. Sijacki[13], J. Silva[126a,126d], Y. Silver[153], S.B. Silverstein[146a], V. Simak[128], O. Simard[5], Lj. Simic[13], S. Simion[117], E. Simioni[83], B. Simmons[78], D. Simon[34], R. Simoniello[91a,91b], P. Sinervo[158], N.B. Sinev[116], M. Sioli[20a,20b], G. Siragusa[174], A.N. Sisakyan[65,*], S.Yu. Sivoklokov[99], J. Sjölin[146a,146b], T.B. Sjursen[14], M.B. Skinner[72], H.P. Skottowe[57], P. Skubic[113], M. Slater[18], T. Slavicek[128], M. Slawinska[107], K. Sliwa[161], V. Smakhtin[172], B.H. Smart[46], L. Smestad[14], S.Yu. Smirnov[98], Y. Smirnov[98], L.N. Smirnova[99,ag], O. Smirnova[81], M.N.K. Smith[35], R.W. Smith[35], M. Smizanska[72], K. Smolek[128], A.A. Snesarev[96], G. Snidero[76], S. Snyder[25], R. Sobie[169,k], F. Socher[44], A. Soffer[153], D.A. Soh[151,af], C.A. Solans[30], M. Solar[128], J. Solc[128], E.Yu. Soldatov[98], U. Soldevila[167], A.A. Solodkov[130], A. Soloshenko[65], O.V. Solovyanov[130], V. Solovyev[123], P. Sommer[48], H.Y. Song[33b], N. Soni[1], A. Sood[15], A. Sopczak[128], B. Sopko[128], V. Sopko[128], V. Sorin[12], D. Sosa[58b], M. Sosebee[8], C.L. Sotiropoulou[124a,124b], R. Soualah[164a,164c], A.M. Soukharev[109,c], D. South[42], B.C. Sowden[77], S. Spagnolo[73a,73b], M. Spalla[124a,124b], F. Spanò[77], W.R. Spearman[57], D. Sperlich[16], F. Spettel[101], R. Spighi[20a], G. Spigo[30], L.A. Spiller[88], M. Spousta[129], T. Spreitzer[158], R.D. St. Denis[53,*], S. Staerz[44], J. Stahlman[122], R. Stamen[58a], S. Stamm[16], E. Stanecka[39], C. Stanescu[134a], M. Stanescu-Bellu[42], M.M. Stanitzki[42], S. Stapnes[119], E.A. Starchenko[130], J. Stark[55], P. Staroba[127], P. Starovoitov[42], R. Staszewski[39], P. Stavina[144a,*], P. Steinberg[25], B. Stelzer[142], H.J. Stelzer[30], O. Stelzer-Chilton[159a], H. Stenzel[52], G.A. Stewart[53], J.A. Stillings[21], M.C. Stockton[87], M. Stoebe[87], G. Stoicea[26a], P. Stolte[54], S. Stonjek[101], A.R. Stradling[8], A. Straessner[44], M.E. Stramaglia[17], J. Strandberg[147], S. Strandberg[146a,146b], A. Strandlie[119], E. Strauss[143], M. Strauss[113], P. Strizenec[144b], R. Ströhmer[174], D.M. Strom[116], R. Stroynowski[40], A. Strubig[106], S.A. Stucci[17], B. Stugu[14], N.A. Styles[42], D. Su[143], J. Su[125], R. Subramaniam[79], A. Succurro[12], Y. Sugaya[118], C. Suhr[108], M. Suk[128], V.V. Sulin[96], S. Sultansoy[4c], T. Sumida[68], S. Sun[57], X. Sun[33a], J.E. Sundermann[48], K. Suruliz[149], G. Susinno[37a,37b], M.R. Sutton[149], S. Suzuki[66], M. Svatos[127], S. Swedish[168], M. Swiatlowski[143], I. Sykora[144a], T. Sykora[129], D. Ta[90], C. Taccini[134a,134b], K. Tackmann[42], J. Taenzer[158], A. Taffard[163], R. Tafirout[159a], N. Taiblum[153], H. Takai[25], R. Takashima[69], H. Takeda[67], T. Takeshita[140], Y. Takubo[66], M. Talby[85], A.A. Talyshev[109,c], J.Y.C. Tam[174], K.G. Tan[88], J. Tanaka[155], R. Tanaka[117], S. Tanaka[66], B.B. Tannenwald[111], N. Tannoury[21], S. Tapprogge[83], S. Tarem[152], F. Tarrade[29],

JHEP08(2016)147

G.F. Tartarelli[91a], P. Tas[129], M. Tasevsky[127], T. Tashiro[68], E. Tassi[37a,37b], A. Tavares Delgado[126a,126b], Y. Tayalati[135d], F.E. Taylor[94], G.N. Taylor[88], W. Taylor[159b], F.A. Teischinger[30], M. Teixeira Dias Castanheira[76], P. Teixeira-Dias[77], K.K. Temming[48], H. Ten Kate[30], P.K. Teng[151], J.J. Teoh[118], F. Tepel[175], S. Terada[66], K. Terashi[155], J. Terron[82], S. Terzo[101], M. Testa[47], R.J. Teuscher[158,k], T. Theveneaux-Pelzer[34], J.P. Thomas[18], J. Thomas-Wilsker[77], E.N. Thompson[35], P.D. Thompson[18], R.J. Thompson[84], A.S. Thompson[53], L.A. Thomsen[176], E. Thomson[122], M. Thomson[28], R.P. Thun[89,*], M.J. Tibbetts[15], R.E. Ticse Torres[85], V.O. Tikhomirov[96,ah], Yu.A. Tikhonov[109,c], S. Timoshenko[98], E. Tiouchichine[85], P. Tipton[176], S. Tisserant[85], K. Todome[157], T. Todorov[5,*], S. Todorova-Nova[129], J. Tojo[70], S. Tokár[144a], K. Tokushuku[66], K. Tollefson[90], E. Tolley[57], L. Tomlinson[84], M. Tomoto[103], L. Tompkins[143,ai], K. Toms[105], E. Torrence[116], H. Torres[142], E. Torró Pastor[167], J. Toth[85,aj], F. Touchard[85], D.R. Tovey[139], T. Trefzger[174], L. Tremblet[30], A. Tricoli[30], I.M. Trigger[159a], S. Trincaz-Duvoid[80], M.F. Tripiana[12], W. Trischuk[158], B. Trocmé[55], C. Troncon[91a], M. Trottier-McDonald[15], M. Trovatelli[169], P. True[90], L. Truong[164a,164c], M. Trzebinski[39], A. Trzupek[39], C. Tsarouchas[30], J.C-L. Tseng[120], P.V. Tsiareshka[92], D. Tsionou[154], G. Tsipolitis[10], N. Tsirintanis[9], S. Tsiskaridze[12], V. Tsiskaridze[48], E.G. Tskhadadze[51a], I.I. Tsukerman[97], V. Tsulaia[15], S. Tsuno[66], D. Tsybychev[148], A. Tudorache[26a], V. Tudorache[26a], A.N. Tuna[122], S.A. Tupputi[20a,20b], S. Turchikhin[99,ag], D. Turecek[128], R. Turra[91a,91b], A.J. Turvey[40], P.M. Tuts[35], A. Tykhonov[49], M. Tylmad[146a,146b], M. Tyndel[131], I. Ueda[155], R. Ueno[29], M. Ughetto[146a,146b], M. Ugland[14], M. Uhlenbrock[21], F. Ukegawa[160], G. Unal[30], A. Undrus[25], G. Unel[163], F.C. Ungaro[48], Y. Unno[66], C. Unverdorben[100], J. Urban[144b], P. Urquijo[88], P. Urrejola[83], G. Usai[8], A. Usanova[62], L. Vacavant[85], V. Vacek[128], B. Vachon[87], C. Valderanis[83], N. Valencic[107], S. Valentinetti[20a,20b], A. Valero[167], L. Valery[12], S. Valkar[129], E. Valladolid Gallego[167], S. Vallecorsa[49], J.A. Valls Ferrer[167], W. Van Den Wollenberg[107], P.C. Van Der Deijl[107], R. van der Geer[107], H. van der Graaf[107], R. Van Der Leeuw[107], N. van Eldik[152], P. van Gemmeren[6], J. Van Nieuwkoop[142], I. van Vulpen[107], M.C. van Woerden[30], M. Vanadia[132a,132b], W. Vandelli[30], R. Vanguri[122], A. Vaniachine[6], F. Vannucci[80], G. Vardanyan[177], R. Vari[132a], E.W. Varnes[7], T. Varol[40], D. Varouchas[80], A. Vartapetian[8], K.E. Varvell[150], F. Vazeille[34], T. Vazquez Schroeder[87], J. Veatch[7], L.M. Veloce[158], F. Veloso[126a,126c], T. Velz[21], S. Veneziano[132a], A. Ventura[73a,73b], D. Ventura[86], M. Venturi[169], N. Venturi[158], A. Venturini[23], V. Vercesi[121a], M. Verducci[132a,132b], W. Verkerke[107], J.C. Vermeulen[107], A. Vest[44], M.C. Vetterli[142,d], O. Viazlo[81], I. Vichou[165], T. Vickey[139], O.E. Vickey Boeriu[139], G.H.A. Viehhauser[120], S. Viel[15], R. Vigne[62], M. Villa[20a,20b], M. Villaplana Perez[91a,91b], E. Vilucchi[47], M.G. Vincter[29], V.B. Vinogradov[65], I. Vivarelli[149], F. Vives Vaque[3], S. Vlachos[10], D. Vladoiu[100], M. Vlasak[128], M. Vogel[32a], P. Vokac[128], G. Volpi[124a,124b], M. Volpi[88], H. von der Schmitt[101], H. von Radziewski[48], E. von Toerne[21], V. Vorobel[129], K. Vorobev[98], M. Vos[167], R. Voss[30], J.H. Vossebeld[74], N. Vranjes[13], M. Vranjes Milosavljevic[13], V. Vrba[127], M. Vreeswijk[107], R. Vuillermet[30], I. Vukotic[31], Z. Vykydal[128], P. Wagner[21], W. Wagner[175], H. Wahlberg[71], S. Wahrmund[44], J. Wakabayashi[103], J. Walder[72], R. Walker[100], W. Walkowiak[141], C. Wang[151], F. Wang[173], H. Wang[15], H. Wang[40], J. Wang[42], J. Wang[33a], K. Wang[87], R. Wang[6], S.M. Wang[151], T. Wang[21], T. Wang[35], X. Wang[176], C. Wanotayaroj[116], A. Warburton[87], C.P. Ward[28], D.R. Wardrope[78], M. Warsinsky[48], A. Washbrook[46], C. Wasicki[42], P.M. Watkins[18], A.T. Watson[18], I.J. Watson[150], M.F. Watson[18], G. Watts[138], S. Watts[84], B.M. Waugh[78], S. Webb[84], M.S. Weber[17], S.W. Weber[174], J.S. Webster[31], A.R. Weidberg[120], B. Weinert[61], J. Weingarten[54], C. Weiser[48], H. Weits[107], P.S. Wells[30], T. Wenaus[25], T. Wengler[30], S. Wenig[30], N. Wermes[21], M. Werner[48], P. Werner[30], M. Wessels[58a], J. Wetter[161], K. Whalen[116], A.M. Wharton[72], A. White[8], M.J. White[1], R. White[32b], S. White[124a,124b], D. Whiteson[163],

JHEP08(2016)147

F.J. Wickens[131], W. Wiedenmann[173], M. Wielers[131], P. Wienemann[21], C. Wiglesworth[36], L.A.M. Wiik-Fuchs[21], A. Wildauer[101], H.G. Wilkens[30], H.H. Williams[122], S. Williams[107], C. Willis[90], S. Willocq[86], A. Wilson[89], J.A. Wilson[18], I. Wingerter-Seez[5], F. Winklmeier[116], B.T. Winter[21], M. Wittgen[143], J. Wittkowski[100], S.J. Wollstadt[83], M.W. Wolter[39], H. Wolters[126a,126c], B.K. Wosiek[39], J. Wotschack[30], M.J. Woudstra[84], K.W. Wozniak[39], M. Wu[55], M. Wu[31], S.L. Wu[173], X. Wu[49], Y. Wu[89], T.R. Wyatt[84], B.M. Wynne[46], S. Xella[36], D. Xu[33a], L. Xu[33b,ak], B. Yabsley[150], S. Yacoob[145a], R. Yakabe[67], M. Yamada[66], Y. Yamaguchi[118], A. Yamamoto[66], S. Yamamoto[155], T. Yamanaka[155], K. Yamauchi[103], Y. Yamazaki[67], Z. Yan[22], H. Yang[33e], H. Yang[173], Y. Yang[151], W-M. Yao[15], Y. Yasu[66], E. Yatsenko[5], K.H. Yau Wong[21], J. Ye[40], S. Ye[25], I. Yeletskikh[65], A.L. Yen[57], E. Yildirim[42], K. Yorita[171], R. Yoshida[6], K. Yoshihara[122], C. Young[143], C.J.S. Young[30], S. Youssef[22], D.R. Yu[15], J. Yu[8], J.M. Yu[89], J. Yu[114], L. Yuan[67], S.P.Y. Yuen[21], A. Yurkewicz[108], I. Yusuff[28,al], B. Zabinski[39], R. Zaidan[63], A.M. Zaitsev[130,ab], J. Zalieckas[14], A. Zaman[148], S. Zambito[57], L. Zanello[132a,132b], D. Zanzi[88], C. Zeitnitz[175], M. Zeman[128], A. Zemla[38a], K. Zengel[23], O. Zenin[130], T. Ženiš[144a], D. Zerwas[117], D. Zhang[89], F. Zhang[173], H. Zhang[33c], J. Zhang[6], L. Zhang[48], R. Zhang[33b], X. Zhang[33d], Z. Zhang[117], X. Zhao[40], Y. Zhao[33d,117], Z. Zhao[33b], A. Zhemchugov[65], J. Zhong[120], B. Zhou[89], C. Zhou[45], L. Zhou[35], L. Zhou[40], N. Zhou[163], C.G. Zhu[33d], H. Zhu[33a], J. Zhu[89], Y. Zhu[33b], X. Zhuang[33a], K. Zhukov[96], A. Zibell[174], D. Zieminska[61], N.I. Zimine[65], C. Zimmermann[83], S. Zimmermann[48], Z. Zinonos[54], M. Zinser[83], M. Ziolkowski[141], L. Živković[13], G. Zobernig[173], A. Zoccoli[20a,20b], M. zur Nedden[16], G. Zurzolo[104a,104b] and L. Zwalinski[30]

[1] *Department of Physics, University of Adelaide, Adelaide, Australia*
[2] *Physics Department, SUNY Albany, Albany NY, United States of America*
[3] *Department of Physics, University of Alberta, Edmonton AB, Canada*
[4] [(a)] *Department of Physics, Ankara University, Ankara;* [(b)] *Istanbul Aydin University, Istanbul;* [(c)] *Division of Physics, TOBB University of Economics and Technology, Ankara, Turkey*
[5] *LAPP, CNRS/IN2P3 and Université Savoie Mont Blanc, Annecy-le-Vieux, France*
[6] *High Energy Physics Division, Argonne National Laboratory, Argonne IL, United States of America*
[7] *Department of Physics, University of Arizona, Tucson AZ, United States of America*
[8] *Department of Physics, The University of Texas at Arlington, Arlington TX, United States of America*
[9] *Physics Department, University of Athens, Athens, Greece*
[10] *Physics Department, National Technical University of Athens, Zografou, Greece*
[11] *Institute of Physics, Azerbaijan Academy of Sciences, Baku, Azerbaijan*
[12] *Institut de Física d'Altes Energies and Departament de Física de la Universitat Autònoma de Barcelona, Barcelona, Spain*
[13] *Institute of Physics, University of Belgrade, Belgrade, Serbia*
[14] *Department for Physics and Technology, University of Bergen, Bergen, Norway*
[15] *Physics Division, Lawrence Berkeley National Laboratory and University of California, Berkeley CA, United States of America*
[16] *Department of Physics, Humboldt University, Berlin, Germany*
[17] *Albert Einstein Center for Fundamental Physics and Laboratory for High Energy Physics, University of Bern, Bern, Switzerland*
[18] *School of Physics and Astronomy, University of Birmingham, Birmingham, United Kingdom*
[19] [(a)] *Department of Physics, Bogazici University, Istanbul;* [(b)] *Department of Physics Engineering, Gaziantep University, Gaziantep;* [(c)] *Department of Physics, Dogus University, Istanbul, Turkey*
[20] [(a)] *INFN Sezione di Bologna;* [(b)] *Dipartimento di Fisica e Astronomia, Università di Bologna, Bologna, Italy*
[21] *Physikalisches Institut, University of Bonn, Bonn, Germany*
[22] *Department of Physics, Boston University, Boston MA, United States of America*
[23] *Department of Physics, Brandeis University, Waltham MA, United States of America*

JHEP08(2016)147

[24] [(a)] Universidade Federal do Rio De Janeiro COPPE/EE/IF, Rio de Janeiro; [(b)] Electrical Circuits Department, Federal University of Juiz de Fora (UFJF), Juiz de Fora; [(c)] Federal University of Sao Joao del Rei (UFSJ), Sao Joao del Rei; [(d)] Instituto de Fisica, Universidade de Sao Paulo, Sao Paulo, Brazil
[25] Physics Department, Brookhaven National Laboratory, Upton NY, United States of America
[26] [(a)] National Institute of Physics and Nuclear Engineering, Bucharest; [(b)] National Institute for Research and Development of Isotopic and Molecular Technologies, Physics Department, Cluj Napoca; [(c)] University Politehnica Bucharest, Bucharest; [(d)] West University in Timisoara, Timisoara, Romania
[27] Departamento de Física, Universidad de Buenos Aires, Buenos Aires, Argentina
[28] Cavendish Laboratory, University of Cambridge, Cambridge, United Kingdom
[29] Department of Physics, Carleton University, Ottawa ON, Canada
[30] CERN, Geneva, Switzerland
[31] Enrico Fermi Institute, University of Chicago, Chicago IL, United States of America
[32] [(a)] Departamento de Física, Pontificia Universidad Católica de Chile, Santiago; [(b)] Departamento de Física, Universidad Técnica Federico Santa María, Valparaíso, Chile
[33] [(a)] Institute of High Energy Physics, Chinese Academy of Sciences, Beijing; [(b)] Department of Modern Physics, University of Science and Technology of China, Anhui; [(c)] Department of Physics, Nanjing University, Jiangsu; [(d)] School of Physics, Shandong University, Shandong; [(e)] Department of Physics and Astronomy, Shanghai Key Laboratory for Particle Physics and Cosmology, Shanghai Jiao Tong University, Shanghai; [(f)] Physics Department, Tsinghua University, Beijing 100084, China
[34] Laboratoire de Physique Corpusculaire, Clermont Université and Université Blaise Pascal and CNRS/IN2P3, Clermont-Ferrand, France
[35] Nevis Laboratory, Columbia University, Irvington NY, United States of America
[36] Niels Bohr Institute, University of Copenhagen, Kobenhavn, Denmark
[37] [(a)] INFN Gruppo Collegato di Cosenza, Laboratori Nazionali di Frascati; [(b)] Dipartimento di Fisica, Università della Calabria, Rende, Italy
[38] [(a)] AGH University of Science and Technology, Faculty of Physics and Applied Computer Science, Krakow; [(b)] Marian Smoluchowski Institute of Physics, Jagiellonian University, Krakow, Poland
[39] Institute of Nuclear Physics Polish Academy of Sciences, Krakow, Poland
[40] Physics Department, Southern Methodist University, Dallas TX, United States of America
[41] Physics Department, University of Texas at Dallas, Richardson TX, United States of America
[42] DESY, Hamburg and Zeuthen, Germany
[43] Institut für Experimentelle Physik IV, Technische Universität Dortmund, Dortmund, Germany
[44] Institut für Kern- und Teilchenphysik, Technische Universität Dresden, Dresden, Germany
[45] Department of Physics, Duke University, Durham NC, United States of America
[46] SUPA - School of Physics and Astronomy, University of Edinburgh, Edinburgh, United Kingdom
[47] INFN Laboratori Nazionali di Frascati, Frascati, Italy
[48] Fakultät für Mathematik und Physik, Albert-Ludwigs-Universität, Freiburg, Germany
[49] Section de Physique, Université de Genève, Geneva, Switzerland
[50] [(a)] INFN Sezione di Genova; [(b)] Dipartimento di Fisica, Università di Genova, Genova, Italy
[51] [(a)] E. Andronikashvili Institute of Physics, Iv. Javakhishvili Tbilisi State University, Tbilisi; [(b)] High Energy Physics Institute, Tbilisi State University, Tbilisi, Georgia
[52] II Physikalisches Institut, Justus-Liebig-Universität Giessen, Giessen, Germany
[53] SUPA - School of Physics and Astronomy, University of Glasgow, Glasgow, United Kingdom
[54] II Physikalisches Institut, Georg-August-Universität, Göttingen, Germany
[55] Laboratoire de Physique Subatomique et de Cosmologie, Université Grenoble-Alpes, CNRS/IN2P3, Grenoble, France
[56] Department of Physics, Hampton University, Hampton VA, United States of America
[57] Laboratory for Particle Physics and Cosmology, Harvard University, Cambridge MA, United States of America

JHEP08(2016)147

[58] [(a)] Kirchhoff-Institut für Physik, Ruprecht-Karls-Universität Heidelberg, Heidelberg; [(b)] Physikalisches Institut, Ruprecht-Karls-Universität Heidelberg, Heidelberg; [(c)] ZITI Institut für technische Informatik, Ruprecht-Karls-Universität Heidelberg, Mannheim, Germany
[59] Faculty of Applied Information Science, Hiroshima Institute of Technology, Hiroshima, Japan
[60] [(a)] Department of Physics, The Chinese University of Hong Kong, Shatin, N.T., Hong Kong; [(b)] Department of Physics, The University of Hong Kong, Hong Kong; [(c)] Department of Physics, The Hong Kong University of Science and Technology, Clear Water Bay, Kowloon, Hong Kong, China
[61] Department of Physics, Indiana University, Bloomington IN, United States of America
[62] Institut für Astro- und Teilchenphysik, Leopold-Franzens-Universität, Innsbruck, Austria
[63] University of Iowa, Iowa City IA, United States of America
[64] Department of Physics and Astronomy, Iowa State University, Ames IA, United States of America
[65] Joint Institute for Nuclear Research, JINR Dubna, Dubna, Russia
[66] KEK, High Energy Accelerator Research Organization, Tsukuba, Japan
[67] Graduate School of Science, Kobe University, Kobe, Japan
[68] Faculty of Science, Kyoto University, Kyoto, Japan
[69] Kyoto University of Education, Kyoto, Japan
[70] Department of Physics, Kyushu University, Fukuoka, Japan
[71] Instituto de Física La Plata, Universidad Nacional de La Plata and CONICET, La Plata, Argentina
[72] Physics Department, Lancaster University, Lancaster, United Kingdom
[73] [(a)] INFN Sezione di Lecce; [(b)] Dipartimento di Matematica e Fisica, Università del Salento, Lecce, Italy
[74] Oliver Lodge Laboratory, University of Liverpool, Liverpool, United Kingdom
[75] Department of Physics, Jožef Stefan Institute and University of Ljubljana, Ljubljana, Slovenia
[76] School of Physics and Astronomy, Queen Mary University of London, London, United Kingdom
[77] Department of Physics, Royal Holloway University of London, Surrey, United Kingdom
[78] Department of Physics and Astronomy, University College London, London, United Kingdom
[79] Louisiana Tech University, Ruston LA, United States of America
[80] Laboratoire de Physique Nucléaire et de Hautes Energies, UPMC and Université Paris-Diderot and CNRS/IN2P3, Paris, France
[81] Fysiska institutionen, Lunds universitet, Lund, Sweden
[82] Departamento de Fisica Teorica C-15, Universidad Autonoma de Madrid, Madrid, Spain
[83] Institut für Physik, Universität Mainz, Mainz, Germany
[84] School of Physics and Astronomy, University of Manchester, Manchester, United Kingdom
[85] CPPM, Aix-Marseille Université and CNRS/IN2P3, Marseille, France
[86] Department of Physics, University of Massachusetts, Amherst MA, United States of America
[87] Department of Physics, McGill University, Montreal QC, Canada
[88] School of Physics, University of Melbourne, Victoria, Australia
[89] Department of Physics, The University of Michigan, Ann Arbor MI, United States of America
[90] Department of Physics and Astronomy, Michigan State University, East Lansing MI, United States of America
[91] [(a)] INFN Sezione di Milano; [(b)] Dipartimento di Fisica, Università di Milano, Milano, Italy
[92] B.I. Stepanov Institute of Physics, National Academy of Sciences of Belarus, Minsk, Republic of Belarus
[93] National Scientific and Educational Centre for Particle and High Energy Physics, Minsk, Republic of Belarus
[94] Department of Physics, Massachusetts Institute of Technology, Cambridge MA, United States of America
[95] Group of Particle Physics, University of Montreal, Montreal QC, Canada
[96] P.N. Lebedev Institute of Physics, Academy of Sciences, Moscow, Russia
[97] Institute for Theoretical and Experimental Physics (ITEP), Moscow, Russia
[98] National Research Nuclear University MEPhI, Moscow, Russia

JHEP08(2016)147

[99] D.V. Skobeltsyn Institute of Nuclear Physics, M.V. Lomonosov Moscow State University, Moscow, Russia
[100] Fakultät für Physik, Ludwig-Maximilians-Universität München, München, Germany
[101] Max-Planck-Institut für Physik (Werner-Heisenberg-Institut), München, Germany
[102] Nagasaki Institute of Applied Science, Nagasaki, Japan
[103] Graduate School of Science and Kobayashi-Maskawa Institute, Nagoya University, Nagoya, Japan
[104] [(a)] INFN Sezione di Napoli; [(b)] Dipartimento di Fisica, Università di Napoli, Napoli, Italy
[105] Department of Physics and Astronomy, University of New Mexico, Albuquerque NM, United States of America
[106] Institute for Mathematics, Astrophysics and Particle Physics, Radboud University Nijmegen/Nikhef, Nijmegen, Netherlands
[107] Nikhef National Institute for Subatomic Physics and University of Amsterdam, Amsterdam, Netherlands
[108] Department of Physics, Northern Illinois University, DeKalb IL, United States of America
[109] Budker Institute of Nuclear Physics, SB RAS, Novosibirsk, Russia
[110] Department of Physics, New York University, New York NY, United States of America
[111] Ohio State University, Columbus OH, United States of America
[112] Faculty of Science, Okayama University, Okayama, Japan
[113] Homer L. Dodge Department of Physics and Astronomy, University of Oklahoma, Norman OK, United States of America
[114] Department of Physics, Oklahoma State University, Stillwater OK, United States of America
[115] Palacký University, RCPTM, Olomouc, Czech Republic
[116] Center for High Energy Physics, University of Oregon, Eugene OR, United States of America
[117] LAL, Université Paris-Sud and CNRS/IN2P3, Orsay, France
[118] Graduate School of Science, Osaka University, Osaka, Japan
[119] Department of Physics, University of Oslo, Oslo, Norway
[120] Department of Physics, Oxford University, Oxford, United Kingdom
[121] [(a)] INFN Sezione di Pavia; [(b)] Dipartimento di Fisica, Università di Pavia, Pavia, Italy
[122] Department of Physics, University of Pennsylvania, Philadelphia PA, United States of America
[123] National Research Centre "Kurchatov Institute" B.P.Konstantinov Petersburg Nuclear Physics Institute, St. Petersburg, Russia
[124] [(a)] INFN Sezione di Pisa; [(b)] Dipartimento di Fisica E. Fermi, Università di Pisa, Pisa, Italy
[125] Department of Physics and Astronomy, University of Pittsburgh, Pittsburgh PA, United States of America
[126] [(a)] Laboratório de Instrumentação e Física Experimental de Partículas - LIP, Lisboa; [(b)] Faculdade de Ciências, Universidade de Lisboa, Lisboa; [(c)] Department of Physics, University of Coimbra, Coimbra; [(d)] Centro de Física Nuclear da Universidade de Lisboa, Lisboa; [(e)] Departamento de Fisica, Universidade do Minho, Braga; [(f)] Departamento de Fisica Teorica y del Cosmos and CAFPE, Universidad de Granada, Granada (Spain); [(g)] Dep Fisica and CEFITEC of Faculdade de Ciencias e Tecnologia, Universidade Nova de Lisboa, Caparica, Portugal
[127] Institute of Physics, Academy of Sciences of the Czech Republic, Praha, Czech Republic
[128] Czech Technical University in Prague, Praha, Czech Republic
[129] Faculty of Mathematics and Physics, Charles University in Prague, Praha, Czech Republic
[130] State Research Center Institute for High Energy Physics, Protvino, Russia
[131] Particle Physics Department, Rutherford Appleton Laboratory, Didcot, United Kingdom
[132] [(a)] INFN Sezione di Roma; [(b)] Dipartimento di Fisica, Sapienza Università di Roma, Roma, Italy
[133] [(a)] INFN Sezione di Roma Tor Vergata; [(b)] Dipartimento di Fisica, Università di Roma Tor Vergata, Roma, Italy
[134] [(a)] INFN Sezione di Roma Tre; [(b)] Dipartimento di Matematica e Fisica, Università Roma Tre, Roma, Italy
[135] [(a)] Faculté des Sciences Ain Chock, Réseau Universitaire de Physique des Hautes Energies - Université Hassan II, Casablanca; [(b)] Centre National de l'Energie des Sciences Techniques Nucleaires, Rabat; [(c)] Faculté des Sciences Semlalia, Université Cadi Ayyad, LPHEA-Marrakech;

JHEP08(2016)147

[d] Faculté des Sciences, Université Mohamed Premier and LPTPM, Oujda; [e] Faculté des sciences, Université Mohammed V-Agdal, Rabat, Morocco
[136] DSM/IRFU (Institut de Recherches sur les Lois Fondamentales de l'Univers), CEA Saclay (Commissariat à l'Energie Atomique et aux Energies Alternatives), Gif-sur-Yvette, France
[137] Santa Cruz Institute for Particle Physics, University of California Santa Cruz, Santa Cruz CA, United States of America
[138] Department of Physics, University of Washington, Seattle WA, United States of America
[139] Department of Physics and Astronomy, University of Sheffield, Sheffield, United Kingdom
[140] Department of Physics, Shinshu University, Nagano, Japan
[141] Fachbereich Physik, Universität Siegen, Siegen, Germany
[142] Department of Physics, Simon Fraser University, Burnaby BC, Canada
[143] SLAC National Accelerator Laboratory, Stanford CA, United States of America
[144] [a] Faculty of Mathematics, Physics & Informatics, Comenius University, Bratislava; [b] Department of Subnuclear Physics, Institute of Experimental Physics of the Slovak Academy of Sciences, Kosice, Slovak Republic
[145] [a] Department of Physics, University of Cape Town, Cape Town; [b] Department of Physics, University of Johannesburg, Johannesburg; [c] School of Physics, University of the Witwatersrand, Johannesburg, South Africa
[146] [a] Department of Physics, Stockholm University; [b] The Oskar Klein Centre, Stockholm, Sweden
[147] Physics Department, Royal Institute of Technology, Stockholm, Sweden
[148] Departments of Physics & Astronomy and Chemistry, Stony Brook University, Stony Brook NY, United States of America
[149] Department of Physics and Astronomy, University of Sussex, Brighton, United Kingdom
[150] School of Physics, University of Sydney, Sydney, Australia
[151] Institute of Physics, Academia Sinica, Taipei, Taiwan
[152] Department of Physics, Technion: Israel Institute of Technology, Haifa, Israel
[153] Raymond and Beverly Sackler School of Physics and Astronomy, Tel Aviv University, Tel Aviv, Israel
[154] Department of Physics, Aristotle University of Thessaloniki, Thessaloniki, Greece
[155] International Center for Elementary Particle Physics and Department of Physics, The University of Tokyo, Tokyo, Japan
[156] Graduate School of Science and Technology, Tokyo Metropolitan University, Tokyo, Japan
[157] Department of Physics, Tokyo Institute of Technology, Tokyo, Japan
[158] Department of Physics, University of Toronto, Toronto ON, Canada
[159] [a] TRIUMF, Vancouver BC; [b] Department of Physics and Astronomy, York University, Toronto ON, Canada
[160] Faculty of Pure and Applied Sciences, University of Tsukuba, Tsukuba, Japan
[161] Department of Physics and Astronomy, Tufts University, Medford MA, United States of America
[162] Centro de Investigaciones, Universidad Antonio Narino, Bogota, Colombia
[163] Department of Physics and Astronomy, University of California Irvine, Irvine CA, United States of America
[164] [a] INFN Gruppo Collegato di Udine, Sezione di Trieste, Udine; [b] ICTP, Trieste; [c] Dipartimento di Chimica, Fisica e Ambiente, Università di Udine, Udine, Italy
[165] Department of Physics, University of Illinois, Urbana IL, United States of America
[166] Department of Physics and Astronomy, University of Uppsala, Uppsala, Sweden
[167] Instituto de Física Corpuscular (IFIC) and Departamento de Física Atómica, Molecular y Nuclear and Departamento de Ingeniería Electrónica and Instituto de Microelectrónica de Barcelona (IMB-CNM), University of Valencia and CSIC, Valencia, Spain
[168] Department of Physics, University of British Columbia, Vancouver BC, Canada
[169] Department of Physics and Astronomy, University of Victoria, Victoria BC, Canada
[170] Department of Physics, University of Warwick, Coventry, United Kingdom
[171] Waseda University, Tokyo, Japan
[172] Department of Particle Physics, The Weizmann Institute of Science, Rehovot, Israel

JHEP08(2016)147

[173] Department of Physics, University of Wisconsin, Madison WI, United States of America
[174] Fakultät für Physik und Astronomie, Julius-Maximilians-Universität, Würzburg, Germany
[175] Fachbereich C Physik, Bergische Universität Wuppertal, Wuppertal, Germany
[176] Department of Physics, Yale University, New Haven CT, United States of America
[177] Yerevan Physics Institute, Yerevan, Armenia
[178] Centre de Calcul de l'Institut National de Physique Nucléaire et de Physique des Particules (IN2P3), Villeurbanne, France

[a] Also at Department of Physics, King's College London, London, United Kingdom
[b] Also at Institute of Physics, Azerbaijan Academy of Sciences, Baku, Azerbaijan
[c] Also at Novosibirsk State University, Novosibirsk, Russia
[d] Also at TRIUMF, Vancouver BC, Canada
[e] Also at Department of Physics, California State University, Fresno CA, United States of America
[f] Also at Department of Physics, University of Fribourg, Fribourg, Switzerland
[g] Also at Departamento de Fisica e Astronomia, Faculdade de Ciencias, Universidade do Porto, Portugal
[h] Also at Tomsk State University, Tomsk, Russia
[i] Also at CPPM, Aix-Marseille Université and CNRS/IN2P3, Marseille, France
[j] Also at Universita di Napoli Parthenope, Napoli, Italy
[k] Also at Institute of Particle Physics (IPP), Canada
[l] Also at Particle Physics Department, Rutherford Appleton Laboratory, Didcot, United Kingdom
[m] Also at Department of Physics, St. Petersburg State Polytechnical University, St. Petersburg, Russia
[n] Also at Louisiana Tech University, Ruston LA, United States of America
[o] Also at Institucio Catalana de Recerca i Estudis Avancats, ICREA, Barcelona, Spain
[p] Also at Graduate School of Science, Osaka University, Osaka, Japan
[q] Also at Department of Physics, National Tsing Hua University, Taiwan
[r] Also at Department of Physics, The University of Texas at Austin, Austin TX, United States of America
[s] Also at Institute of Theoretical Physics, Ilia State University, Tbilisi, Georgia
[t] Also at CERN, Geneva, Switzerland
[u] Also at Georgian Technical University (GTU),Tbilisi, Georgia
[v] Also at Manhattan College, New York NY, United States of America
[w] Also at Hellenic Open University, Patras, Greece
[x] Also at Institute of Physics, Academia Sinica, Taipei, Taiwan
[y] Also at LAL, Université Paris-Sud and CNRS/IN2P3, Orsay, France
[z] Also at Academia Sinica Grid Computing, Institute of Physics, Academia Sinica, Taipei, Taiwan
[aa] Also at School of Physics, Shandong University, Shandong, China
[ab] Also at Moscow Institute of Physics and Technology State University, Dolgoprudny, Russia
[ac] Also at Section de Physique, Université de Genève, Geneva, Switzerland
[ad] Also at International School for Advanced Studies (SISSA), Trieste, Italy
[ae] Also at Department of Physics and Astronomy, University of South Carolina, Columbia SC, United States of America
[af] Also at School of Physics and Engineering, Sun Yat-sen University, Guangzhou, China
[ag] Also at Faculty of Physics, M.V.Lomonosov Moscow State University, Moscow, Russia
[ah] Also at National Research Nuclear University MEPhI, Moscow, Russia
[ai] Also at Department of Physics, Stanford University, Stanford CA, United States of America
[aj] Also at Institute for Particle and Nuclear Physics, Wigner Research Centre for Physics, Budapest, Hungary
[ak] Also at Department of Physics, The University of Michigan, Ann Arbor MI, United States of America
[al] Also at University of Malaya, Department of Physics, Kuala Lumpur, Malaysia
[*] Deceased

JHEP08(2016)147